Up-scaled production and differentiation of chondrogenic aggregates for endochondral bone regeneration

Andrea García González
7120656

Supervised by:
Flurina Staubli, MSc

Examiner:
Dr. ir. Debby Gawlitta

Second Examiner:
Dr. Mylène de Ruijter

Master of Science in Regenerative Medicine and Technology
September 2023

Abstract

Chondrogenic aggregates have emerged as promising building blocks for the development of implants intended to facilitate bone defect regeneration through the endochondral bone regeneration process. While most protocols rely on static culture systems to create these cell aggregates, scalability limitations have impeded their broader application. In this regard, dynamic culture systems offer an advantageous approach by enabling automated aggregate production, which not only ensures scalability and workload reduction but also aligns with good manufacturing practices (GMP) and facilitate clinical translation. In this study, we investigated the feasibility of collision-based self-assembly of human bone marrow-derived mesenchymal stromal cell (hBM-MSC) aggregates and their subsequent chondrogenic differentiation within the same spinner flask setup. Moreover, qualitative analyses of neural cell adhesion molecule (NCAM) protein expression were performed to study the effect of the hydrodynamic environment on cell aggregation in comparison to static culture. Given that stirring rate influences cell-cell collisions, in this study different velocities of the spinner flask were examined to determine the most favourable one for spontaneous hBM-MSC aggregate formation. The identification of appropriate stirring rate allowed dynamic spinner flask culture ($1x10^6$ cells/mL) of the spontaneously formed aggregates for up to 21 days using two different donors. Dynamically cultured aggregates showed significant variation in aggregates size and shape as opposed to static culture. Importantly, dynamic culture did not affect aggregate viability, although cell death was observed due to the large size of the aggregates. When assessing cell differentiation, staining of dynamically cultured aggregate sections for glycosaminoglycans (GAGs) and collagen II showed inter- and intra-aggregate heterogeneity in comparison to static culture. Moreover, NCAM protein expression was not modulated by the hydrodynamic environment, although reduction on its expression was observed in chondrogenically differentiated cells within the aggregates. Hence, our work demonstrated that collision-based formation of aggregates and their subsequent chondrogenic differentiation within the same dynamic culture system was possible. However, the observation of considerable heterogeneity in dynamic culture highlights the need for further exploration to unravel the underlying molecular mechanisms governing these variations.

Key words

Spinner flask, endochondral ossification, mesenchymal stromal cells, chondrogenic differentiation, bone regeneration

Layman's summary

Chondrogenic aggregates, which are a group of cells that stick together and are able to produce cartilage template, can be used to create implants that are placed in bone fractures in order to heal bone. These aggregates are most often created by using a specific stem cell type that can be derived from the bone marrow, which are mesenchymal stromal cells. These cells are able to form aggregates spontaneously. Besides, when exposed to different factors, cells can become specialized and turn into chondrocytes, which are the cells forming the cartilage. To form this chondrogenic aggregates in the laboratory, static culture systems are used. An example of these systems are plates with wells, where in each well an aggregate is formed. However, this formation process is time-consuming and requires a lot of work, therefore making it difficult to make large amounts of aggregates. To overcome these limitations, dynamic culture systems may be used, such as spinner flasks, which are flasks that have a mixing system that generates fluid flow inside them. When cells are put inside the flasks, the fluid flow makes cells collide, and that is how aggregates are formed. Using this system, a lot of aggregates can be formed within the same flask, which reduces the labour intensity and makes it easier to scale up the production and, in the end, more suitable for medical use.

In our study, we explored a way to create these aggregates and then make them chondrogenic within the same spinner flask. Besides, we wanted to study how this dynamic environment affected the process of cell aggregation in comparison to the static culture. To do so, we studied a protein involved in cell aggregation, which is called neural cell adhesion molecule (NCAM). First, we tested different speeds in order to see which one was the best to allow the formation of these cell aggregates. Once we found a useful speed, we kept the aggregates for 21 days inside the spinner flask in order to see if we could make them become chondrogenic. Our results successfully showed that it was possible. However, the size and shape of the aggregates obtained were highly variable. Moreover, not all the parts of the aggregates became chondrogenic in comparison to the ones cultured statically. Regarding NCAM, the spinning environment did not change the amount of this protein, but cells that were becoming chondrocytes had less amount of it.

In conclusion, we could demonstrate that chondrogenic aggregates could be form thanks to the collision of single cells inside the spinner flask. However, the aggregates obtained were variable in terms of size and shape in comparison to the static culture. Additionally, production of cartilage of the cells was variable. Therefore, more research need to be carried out to understand why this happens at the molecular level. Still, this study advances our knowledge of making cartilage and paves the way for better treatments for bone damage in the future.

Index

Introduction

In the context of bone formation and fracture healing, two main mechanisms govern these processes, which are intramembranous ossification and endochondral ossification[1,2]. The former involves the differentiation of mesenchymal stem cells into osteoblasts so as to form bone. In contrast, in the latter, these stem cells undergo differentiation into chondrocytes, leading to the formation of a hyaline cartilage matrix. Subsequently, osteoblasts infiltrate the matrix and initiate osteoid production, eventually transforming cartilage into bone[2].

During fracture healing, a series of orchestrated events come into play. Mesenchymal stem cells are recruited to the bone fracture by chemotaxis, where they proliferate and differentiate into chondrocytes, which secrete a cartilaginous matrix that forms the soft callus[2,3]. At a later time, the hypertrophic chondrocytes present in the callus secrete bioactive factors that allow the invasion of blood vessels, subsequent extravasation of osteoblasts and, ultimately, remodelling of the cartilaginous tissue into bone[1,2].

Despite the inherent ability of bone to regenerate, bone injuries may be unable to resolve on their own and need medical support from the scope of tissue engineering[4]. Latterly, endochondral bone regeneration, which mimics endochondral ossification, has gained significance in the field of regenerative medicine as a potential approach for addressing the treatment of bone defects[4]. In this regard, multipotent mesenchymal stromal cells (MSCs) have been employed due to their ability to undergo *in vitro* differentiation into the chondrocyte, osteoblast, and adipocyte lineages[5].

Aiming to mimic endochondral ossification in the laboratory, several research groups have used *in vitro* generated cartilage with successful bone formation *in vivo*[6–8]. As an example, Longoni and colleagues used an approach based on chondrogenic aggregates derived from allogeneic MSCs. In their study, these aggregates were differentiated towards the chondrogenic lineage in an *in vitro* static culture prior to implantation *in vivo*, where they were successfully remodelled into bone[6].

Due to the inherent self-assembly capability of MSCs in three-dimensional (3D) aggregates[9,10], the implementation of 3D cultures has become extensively employed in the field of regenerative medicine and tissue engineering. By recapitulating the cellular microenvironment found *in vivo*, these cultures offer significant benefits, including enhanced cell-to-cell interactions and communication, as well as cell-to-extracellular matrix (ECM) interactions[9,11,12]. Moreover, the presence of biochemical stimuli influences cellular properties and behaviour (e.g., phenotype, function, and viability)[12,13], while preserving the potential for cell differentiation[14]. In endochondral bone regeneration, most protocols for chondrogenic culture of MSC aggregates rely on 3D static culture methods. Among these, a widely utilized approach is low-adhesion surfaces (e.g., low-adhesion 96 well-plates), where aggregates form thanks to the promotion of cell-cell interactions which are maximized by cell proximity after centrifugation[15–17]. Despite their effectiveness and simple protocol of preparation, they present challenges in terms of clinical translation due to the time-consuming nature and lack of scalability of the generative process[15]. These problems are related to the individualized cell handling and medium exchange[15], which increase the workload and the risk of contamination, and may introduce variability in conditions among samples. Hence, there is an urge to explore alternative approaches that enable an automated production of these cell aggregates, thereby allowing scalability, workload reduction, and ensuring consistency in MSC aggregate formation and differentiation.

Dynamic culture systems (i.e., bioreactors) have emerged as a commonly employed solution for scaling up the culture process. These systems are based on the collision of single cells due to

continuous stirring, which promotes cell aggregation[15,18]. Furthermore, they offer several advantages over static culture, including homogeneous distribution of oxygen, nutrients, and metabolites[13], along with the presence of mechanical stimuli that can influence cell phenotype[10,13], potentially leading to enhanced cellular differentiation[12,19]. As a result, bioreactors have been used for scaling up expansion, aggregation, and differentiation of stem and stromal cells into different lineages (e.g., chondrogenic, hepatic, etc.)[4,20,21]. The occurrence of expansion and differentiation within the same vessel makes this culture system advantageous over the static culture, since it facilitates automation, good manufacturing practice (GMP)-compliance, and upscaling[15,22]. Rotating wall vessels, spinner flasks, shaking flasks, and perfusion bioreactors are commonly employed bioreactors in dynamic cell culture[9,15,17,23].

The hydrodynamic environment created by the mixing systems within the bioreactors has an impact on the shear forces acting on the cells and the frequency of collisions between cells[18]. In turn, this can affect the aggregation, metabolism, and cellular phenotype of MSCs[9,24]. Shear stress acts as a mechanical cue that alters the expression of genes associated with chondrogenic differentiation[4,15]. However, excessively high shear stress levels can lead to cell membrane disruption and subsequent cell death[4,15,19,23]. On the contrary, excessively low shear stress levels result in the formation of

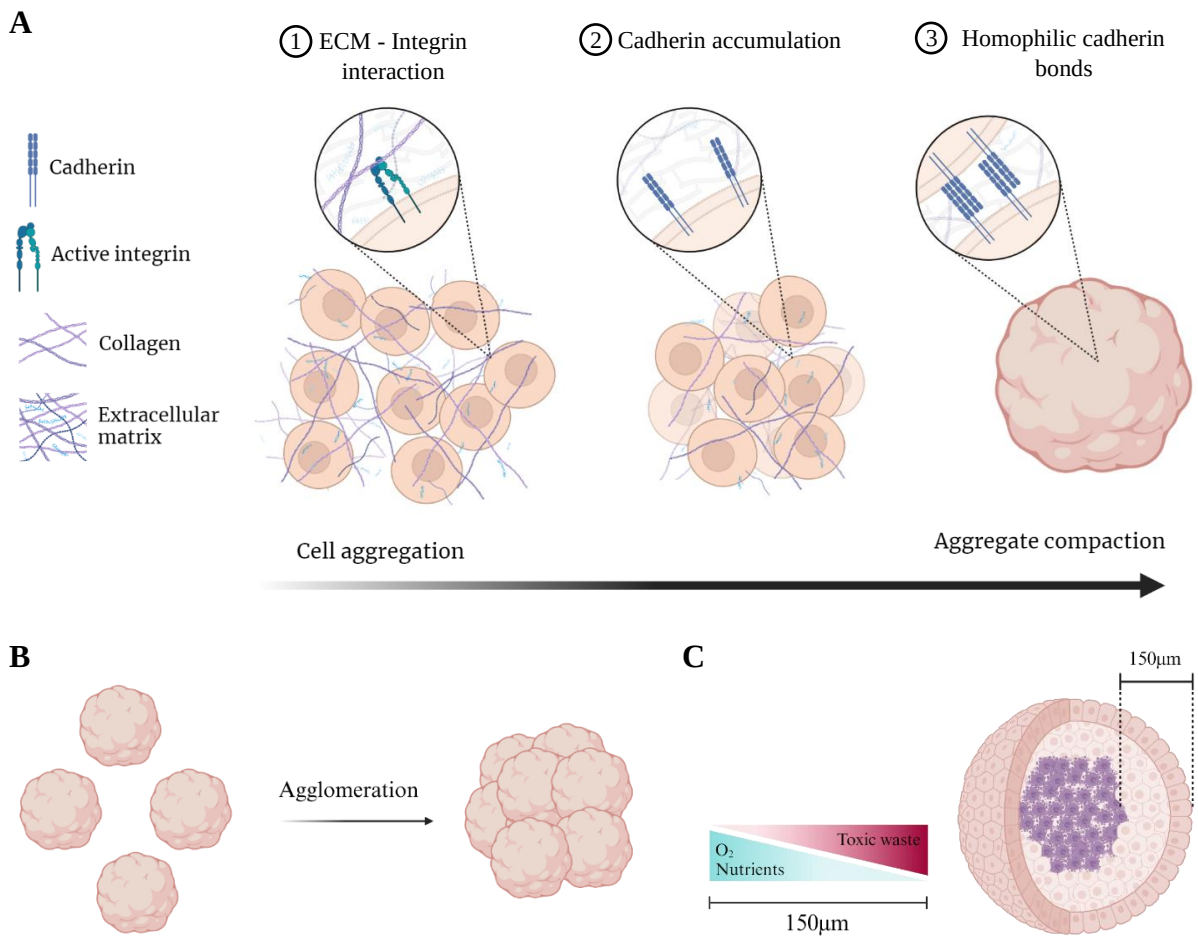

Figure 1. Mesenchymal stromal cell (MSC) aggregate formation process. **(A)** Initially, individual cells are drawn together due to interactions between integrins and the extracellular matrix (ECM). Subsequently, the expression and accumulation of cadherins on the cell surface takes place, leading to a final step of homophilic binding between cadherins. As a result, compact MSC aggregates are formed. **(B)** Under specific conditions, aggregates can fuse, resulting in cell agglomerates. **(C)** In aggregates or agglomerates whose surface-to-centre distance exceeds 150µm, a necrotic core may develop due to accumulation of toxic debris and limited or no diffusion of oxygen and nutrients. Images were created with BioRender and based on Kinney *et al*. (2011)[9], Cui *et al*. (2017)[23], and Kouroupis and Correa (2021)[16].

agglomerates composed of individual aggregates (Figure 1B)[4,9,15], which compromises the viability and differentiation capacity of these aggregates[15]. This occurs due to the creation of a necrotic core, formed by accumulated toxic waste, caused by limited diffusion of oxygen and nutrients[16,23]. Typically, in MSC aggregates the diffusion limit for most small molecules is around 150-200μm[9,16,23,25], and beyond this limit, the formation of a necrotic core occurs (Figure 1C). It is important to note, however, that this limit is applicable under purely diffusive conditions[9], and dynamic culture systems may exhibit variations in this regard[26].

Regarding cell-cell collisions, they play a crucial role in the self-assembly of MSCs into cellular aggregates in dynamic culture. This is because close contact between cells is essential for the formation of these aggregates. The aggregation process takes place in three steps (Figure 1A)[10,16,17,23,25], and is mediated by different adhesion molecules. Initially, single cells form loose aggregates through linkage between arginine-glycine-aspartate (RGD) motifs of the ECM and the integrins present on the membrane of the MSCs. Subsequently, as intercellular interactions increase due to the initial aggregation, cadherin expression is upregulated. Consequently, cadherins accumulate in the cell membrane. Finally, compact MSC aggregates are formed through homophilic bonds established between cadherins. In addition to cadherins, neural cell adhesion molecules (NCAMs) are also an important element for the stabilisation of these aggregates and the maintenance of their condensation[27].

Table I. Comparison of the advantages and disadvantages of different bioreactors used for dynamic cell culture.

Vessel	Advantages	Disadvantages
Rotating wall vessel[17,19,28]	✓ Low turbulence.	x Risk of agglomeration. x Not efficient nutrient and oxygen delivery. x Not scalable.
Spinner flask[19,29]	✓ Less risk of agglomeration. ✓ Efficient nutrient and oxygen delivery. ✓ Easily scalable.	x High shear stress may compromise cell viability.
Shaking flask[15]	✓ Cheap. ✓ Low turbulence.	x Risk of agglomeration. x Not efficient nutrient and oxygen delivery. x Not scalable.
Perfusion bioreactor[15,19,29]	✓ Easy monitoring and control of culture conditions. ✓ Efficient nutrient and oxygen delivery.	x Very expensive. x High shear stress may compromise cell viability.

So as to regulate the hydrodynamic environment and effectively control cell aggregation, several parameters must be considered. These include the type of bioreactor, stirring rate and inoculation cell density[9]. When evaluating the advantages and disadvantages associated with each type of bioreactor (Table I), the spinner flask comes out to be the best choice for upscaling aggregate formation. Going into detail, despite not being scalable, rotating wall vessel and shaking flask generate a hydrodynamic environment that offers low turbulence, which reduces shear stress and, in

turn, does not compromise cell viability. However, this low shear stress environment can derivate in agglomerate formation, and inefficient mass transfer[15,17,28]. On the contrary, despite the possibility of affecting cellular viability[29], shear forces generated by the hydrodynamic environment of the spinner flask may avoid agglomeration and enhance cellular differentiation[10,13]. Additionally, this type of bioreactor offers even dispersion of nutrients and oxygen (which can potentially prevent necrotic core formation)[12,15,30], and it is useful for upscaling[19,29]. Although the perfusion bioreactor could also be a good choice due to its similarities to the spinner flask[15,19,29], its high cost makes it less practical for utilization.

Table II. Comparison of parameters used by different studies for the dynamic culture of MSC aggregates.

Reference	Cell source	Initial cell density	Stirring rate	Bioreactor type	Inoculation
(Frith *et al*., 2010)[12]	hBM-MSCs	$2x10^4$ cells/mL Cells per aggregate unknown.	30	Spinner flask	Pre-formed aggregate inoculation.[a]
(Bhang *et al*., 2011)[30]	hAD-MSCs	$6x10^5$ cells/mL	70	Spinner flask	Single cell inoculation.
(Kwon *et al*., 2015)[31]	hADSCs	$1x10^6$ cells/mL	70	Spinner flask	Single cell inoculation.
(Santos *et al*., 2015)[21]	hUC-MSCs	$1x10^6$ cells/mL	80 (formation) 110 (culture)	Spinner flask, ball impeller	Single cell inoculation.
(He *et al*., 2019)[13]	rBM-MSCs	$2x10^5$ cells/mL $4x10^5$ cells/mL $8x10^5$ cells/mL	40, 45, 50	Spinner flask	Single cell inoculation.
(Miranda *et a*l., 2019)[11]	hUC-MSCs	$1x10^6$ cells/mL	80 (formation) 110 (culture)	Spinner flask, ball impeller	Single cell inoculation.
(Allen *et al*., 2019)[32]	hSyF-MSCs	$5x10^4$ cells/mL	80	Spinner flask, squared impeller	Single cell inoculation.
(Loverdou *et al*., 2022)[4]	hPDCs	$2.5x10^5$ cells/mL 250 cells/aggregate	67, 124, 191	Mini-bioreactors.	Pre-formed aggregate inoculation.[b]

hBM-MSCs: human bone marrow-derived mesenchymal stromal cells; hADSCs: human adipose-derived stromal cells; hUC-MSCs: human umbilical cord tissue-derived mesenchymal stromal cells; rBM-MSCs: rabbit bone marrow-derived mesenchymal stromal cells; hSyF-MSCs: human synovial fluid-derived mesenchymal stromal cells; hPDCs: human periosteum derived cells.

[a] Prior to inoculation, $1x10^6$ cells/mL were cultured for 6 hours in a nonadherent plate and pipetted into smaller aggregates[12].

[b] Prior to inoculation, 250 cells/microwell were cultured for 2 days in a 24 well-plate containing approximately 2000 microwells [4].

As previously mentioned, high shear stress levels can lead to cell death. To avoid this, the stirring rate of the impeller present in the spinner flask can be adjusted, as it directly affects the level of shear stress[9,15]. In other words, the lower the speed, the less shear stress will be produced, and vice versa. Yet, cell aggregation not only depends on the shear stress generated by the hydrodynamic environment, but also on the adhesive strength of the cell adhesion molecules and, consequently, on

the type of cells[18]. This is to say that the level of shear stress necessary to disrupt aggregates or allow agglomeration varies across different bioreactor setups, which generate different hydrodynamic environments, and cell types, which present different adhesion molecule expression profiles. Consequently, so as to know the value of shear stress levels affecting cell aggregation it is necessary to perform computational analysis[4,33,34]. The initial cell density inoculated is also of major importance, since the higher it is, the greater the occurrence of cell-cell collisions, making aggregate formation more frequent[9,18]. Nonetheless, there is a delicate balance between the density necessary for self-aggregation of MSCs and the density that leads to excessive agglomeration resulting in necrotic cores and, consequently, compromising the aggregate potential to differentiate chondrogenically[9,18].

Several studies have successfully achieved self-aggregation of MSCs in spinner flasks (Table II) [11,13,21,30–32]. However, there is no consensus on the initial cell density (ranging from $2x10^4$ cells/mL to $1x10^6$ cells/mL) or stirring rate used (ranging from 30rpm to 110rpm). Furthermore, the possibility of aggregate differentiation into the chondrogenic lineage within a stirred culture has recently been demonstrated[4], although in this case aggregates obtained in microwells were inoculated (250 cells/aggregate). Still, the combined use of spinner flasks for self-aggregation and differentiation of MSC aggregates into the chondrogenic lineage has not been explored yet.

Hence, the aim of this report is to evaluate the feasibility of generating human bone marrow-derived MSC (hBM-MSC) aggregates and inducing their subsequent chondrogenic differentiation after inoculation of single cells in a spinner flask. Furthermore, we aim to qualitatively assess any variations in the expression of the adhesion molecule NCAM in comparison to static culture conditions so as to examine possible differences in aggregate compaction.

Materials and methods

Experimental design and overview

This proof of concept was aimed at the self-aggregation of human bone marrow-derived mesenchymal stromal cells (hBM-MSCs) and the chondrogenic differentiation of the resulting aggregates within a dynamic culture environment. To do so, two culture conditions were used: static culture in a 96 well-plate ($1x10^5$ cells/well), which served as a control, and dynamic culture in a spinner flask ($1x10^6$ cells/mL). Initially, three trials were conducted to test different stirring rates over a 7-day period to assess the formation of hBM-MSC aggregates. Following the identification of a promising stirring speed, a fourth trial was carried out using hBM-MSCs from donor 55. The objective was to determine whether hBM-MSC aggregates could be maintained in dynamic culture for 21 days and achieve chondrogenic differentiation. Subsequently, the same experimental procedure was replicated in a fifth trial using cells from donor 53, enabling the observation of inter-donor variability. During the course of the latter trial, the expression of the adhesion molecule NCAM was qualitatively evaluated.

Expansion of human bone marrow-derived MSCs

For this study, hMSCs were previously isolated from bone marrow aspirates of three donors (MSC53: 20 years old, MSC55: 63 years old, MSC59: 20 years old) as described elsewhere[35]. The procedure was conducted after informed consent and in accordance with the protocol approved by the Medical Ethics Committee (University Medical Center Utrecht). Cells were cultured in MSC

expansion medium comprising α-MEM (22561, Gibco) supplemented with 10% heat-inactivated foetal bovine serum (FBS) (S14068S1810, Biowest), an antibiotic solution consisting of 100units/mL penicillin and 100μg/mL streptomycin (15140, Gibco), 0.2mM L-ascorbic acid 2-phosphate (A8960, Sigma-Aldrich), and 1ng/mL basic fibroblast growth factor (233-FB; R&D Systems).

Cell culture was performed in standard T175 culture flasks (660175, Greiner) at 37ºC and 5% CO_2 under humidified conditions. Expansion medium was changed 2 times per week until reaching 80% confluency, when cells were harvested using 0.25% Trypsin-EDTA (25200072, Gibco). Briefly, cells were washed with PBS and subsequently incubated with 0.25% Trypsin-EDTA for 7 minutes at 37ºC. After this, cells were collected using MSC expansion medium and centrifuged at 320*g* for 5 minutes at room temperature. Supernatant was aspirated and cells were resuspended in MSC expansion medium. Cells were counted using TC20™ Automated Cell Counter (1450102, Bio-Rad) and Trypan Blue solution (T8154, Sigma Aldrich) before passaging and before inoculation into the spinner flask or the well plate.

hBM-MSC aggregates formation and differentiation in spinner flasks

At passage 3, hBM-MSCs were harvested from the T175 flasks and differentiated into the chondrogenic lineage for 21 days. Serum free chondrogenic medium was used during the cell culture, which was composed of high glucose Dulbecco's Modified Eagle Medium (DMEM) (31966, Gibco) supplemented with 1% antibiotic (100units/mL penicillin and 100μg/mL streptomycin), 0.2mM L-ascorbic acid-2-phosphate, 0.1μM dexamethasone (D8893, Sigma-Aldrich), 1% insulin-transferrin-selenium (ITS) + premix (354352, Corning), and 10ng/mL TGF-β1 (100-21, Peprotech).

For dynamic culture, single cell suspensions were seeded in disposable 125mL spinner flasks (3152, Corning) at a concentration of $1x10^6$ cells/mL. Stirring rate was set at a lower speed to promote aggregate formation and cells were incubated at 37ºC and 5% CO_2 under humidified conditions. Aggregates size was checked once a day. Once hBM-MSC aggregates were formed, stirring rate was adjusted to a higher speed to avoid agglomeration of individual aggregates. Parameters regarding working volume, stirring rate and chondrogenic medium change are specified in Table III and Table IV, given that they were variable depending on the trial. Half (50%) medium changes were carried out so that the amount of materials used (e.g., medium, growth factors, etc.) during the 21 days of culture was comparable to that used previously in static culture (i.e., $1x10^6$ cells/aggregate cultured in 400μL of serum free chondrogenic medium, full medium change 2 times per week)[35].

Table III. Parameters used during the 7-day aggregate formation assessment period. Only dynamic culture was used.

	Trial 1	Trial 2	Trial 3
Donor	59	55	55
Working volume	25mL	40mL	40mL
Stirring rate	50 rpm until day 2 80 rpm until day 7	80 rpm until day 2 110 rpm until day 7	100 rpm until day 2 130 rpm until day 7
Chondrogenic medium change	50% medium change at day 3	50% medium change at day 3	50% medium change at day 3

Table IV. Parameters used during the 21-day period of aggregation and differentiation of hBM-MSCs in dynamic culture.

	Trial 4	Trial 5
Donor	55	53
Working volume	44mL	60mL
Stirring rate	80 rpm until day 7 110 rpm until day 21	80 rpm until day 2 110 rpm until day 21
Chondrogenic medium change	50% medium change, twice a week	50% medium change, daily during the first 3 days, and afterwards twice a week

For the static culture used in trials 4 and 5, donors 55 and 53 were used, respectively. In this case, $1x10^5$ cells were seeded per well in a 96 U well suspension culture plate (650185, Greiner) in 100µL of serum free chondrogenic medium. Once cell suspension was seeded, the plates were centrifuged at 320*g* during 5 minutes at room temperature. As spinner flasks, well-plates were maintained inside the incubator during 21 days at 37ºC and 5% CO_2 under humidified conditions. The medium was completely changed according to the frequency specified in Table IV. Additionally, in order to examine the influence of 50% medium changes on the process of chondrogenic differentiation, a static culture was used during the fifth trial. In this case, $1x10^5$ cells were seeded per well in an ultra-low attachment 96 well-plate in 100µL of serum free chondrogenic medium, which was changed as specified in Table IV. Same culture conditions were applied as for the static culture with full medium changes.

Microscopic evaluation of hBM-MSC aggregates

hBM-MSC aggregate size and shape, and aggregate formation were assessed microscopically throughout the cell culture. To do so, 1mL samples collected from the spinner flask were added to a 24 well-plate (662160, Greiner) and visualized using a brightfield microscope (EVOS™ FL Digital Inverted Fluorescence Microscope, Invitrogen). For practical purposes, the size of aggregates was evaluated based on their projected area in square millimetres (mm^2). By way of comparison, spherical aggregates with radii of 150µm and 200µm (close to the diffusion limit) would correspond to projected areas of 0.071mm^2 and 0.126mm^2, respectively. ImageJ software (version 1.53T) was employed to estimate the projected area and the roundness of the hBM-MSC aggregates. To measure roundness, equation (1) was used, where values ranged from 0.0 (denoting a straight line) to 1.0 (denoting a perfect circle). Coefficient of variation (CV) was calculated following equation (2) and expressed as percentage. At least 6 aggregates from the static culture and 10 aggregates from the dynamic culture were analysed per timepoint.

$$\text{Roundness} = \frac{4 \cdot \text{Projected area}}{\pi \cdot \text{Major axis}^2} \quad (1)$$

$$\text{Coefficient of variation (\%)} = \frac{\text{Standard deviation}}{\text{Mean}} \text{ x } 100 \quad (2)$$

Cell viability

Regarding cell viability, prior to performing the assay, single cells and hBM-MSC aggregates smaller than 400μm in size required pre-treatment in order to facilitate their visualization. Namely, being embedded in a collagen matrix. To do so, 1mL of cell suspension was taken from the spinner flask and centrifuged at 320*g* for 5 minutes at room temperature. After aspirating the supernatant, cells were carefully resuspended in MSC expansion medium. Resuspended cells were mixed with 4mg/mL rat tail collagen I (354249, Corning), which was neutralized using 1M NaOH in 10X PBS and incubated for 30 minutes at 37ºC in order to crosslink. To assess cell viability, LIVE/DEAD™ Viability/Cytotoxicity Kit (L3224, Invitrogen) was used following the manufacturers description. Briefly, the collagen matrix containing the cells, and hBM-MSC aggregates from both dynamic and static culture were rinsed in PBS and incubated for 30 minutes with the staining solution (2μL ethidium homodimer (E1169, Invitrogen) and 0.5μL calcein, AM (C3100MP, Invitrogen) in 1mL PBS). After three washes with PBS for 5 minutes to remove the staining solution, samples were imaged using a fluorescence microscope (Leica DMi8 with THUNDER Imaging System, Leica Microsystems).

Histological analyses

In order to carry out histological analyses, the samples had to be embedded in paraffin beforehand. Briefly, following fixation in 4% formaldehyde solution at room temperature, hBM-MSC aggregates underwent dehydration using a sequence of increasing concentrations of ethanol solutions (ranging from 70% to 100%) and were cleared using xylene. Afterwards, hBM-MSC aggregates were paraffin-embedded and 5μm sections were cut using Leica HistoCore BIOCUT microtome (14051756235, Leica Biosystems). In order to be stained, these sections were previously deparaffinized with xylene and gradually rehydrated with decreasing concentrations of ethanol (ranging from 100% to 70%).

To identify the glycosaminoglycans (GAGs), rehydrated samples were stained with 0.4% Toluidine Blue O solution (pH 4.0, T3260, Sigma-Aldrich) for 10 minutes and counterstained with 0.2% Fast Green FCF solution (F7252, Sigma-Aldrich) for 3 minutes. Samples were dehydrated as stated earlier and mounted using Eukitt® Quick-hardening mounting medium (03989, Sigma-Aldrich). Toluidine Blue stained the GAGs, while Fast Green stained the collagenous fibres and cytoplasm.

To detect collagen type II, rehydrated samples were initially incubated for 10 minutes with 0.3% H_2O_2 so as to block peroxidase activity. Subsequently, antigens were retrieved by sequential incubation of the samples with 1mg/mL pronase (11459643001, Roche) and 10mg/mL hyaluronidase (H2126, Sigma-Aldrich) for 30 minutes at 37ºC each. After a blocking step using 5% BSA/PBS, samples were cultured overnight at 4ºC with the primary antibody against collagen type II (1:100 dilution, clone II-II6B3, Developmental Studies Hybridoma Bank). The incubation with the secondary antibody BrightVision goat anti-mouse IgG HRP (VWRKDPVM110HRP, Immunologic) was performed afterwards for 1 hour at room temperature. Following the application of DAB peroxidase substrate solution (SK-4100, Vector Laboratories) until a brown background was observed, nuclei were counterstained with Mayer's Haematoxylin, Q-Path® (10047105, VWR Chemicals). Samples were posteriorly dehydrated as mentioned before and mounted with Eukitt® Quick-hardening mounting medium (03989, Sigma-Aldrich). Mouse IgG1 (1:100 dilution, X0931, Dako) was used as a negative control.

Immunofluorescence analysis

For immunofluorescence analysis, hBM-MSC aggregates were fixed and maintained in 4% formaldehyde solution at room temperature until being embedded in paraffin as described before. 5µm sections obtained from paraffin embedded hBM-MSC aggregates were deparaffinated and rehydrated as previously mentioned. Afterwards, immunofluorescence staining was conducted. In brief, heat-based antigen retrieval was performed using 10mM citrate buffer (pH 6.0) at 95ºC for 20 minutes, followed by a blocking step for 1h at room temperature using 22.25mg/mL glycine (1.04201, Millipore) in 5% BSA/PBS. Posteriorly, samples were incubated overnight at 4ºC with CD56 (NCAM) eFluor® 660 antibody (1:25 dilution, 50-0565-80, clone 5tukon56, Invitrogen) diluted in 5% BSA/PBS. Finally, nuclei were counterstained and coverslips were mounted using VECTASHIELD® HardSet Antifade Mounting Medium with DAPI (H-1500, Vector Laboratories). The immunofluorescence signals were imaged using a fluorescence microscope (Leica DMi8 with THUNDER Imaging System, Leica Microsystems).

Biochemical analyses

For GAGs and DNA quantification, samples were first digested overnight at 60ºC in papain digestion buffer, composed by 7.75units/mL papain (P3125, Sigma Aldrich), 0.2M NaH_2PO_4, 0.1 EDTA.$2H_2O$, and 1.57mg/mL DL-cysteine hydrochloride (C9768, Sigma Aldrich).

In order to detect the total content of GAGs per aggregate, a DMMB assay was used. To create the standard curve, 10µg/mL chondroitin sulphate (C4384, Sigma Aldrich) in PBS-EDTA was serially diluted at a 1:2 ratio. 100µL of sample dilutions in PBS-EDTA (ranging from 1:20 to 1:150) and chondroitin sulphate dilutions were pipetted in duplicate into a 96 F-bottom well polystyrene plate (655101, Greiner). After adding 200µL of 1,9-dimethyl-methylene blue solution (pH 6.5, 341088, Sigma Aldrich) per well, absorbance was measured at 525nm and 595nm. From there, the overall content of GAGs per aggregate was quantified.

GAG levels were corrected for DNA content. Quant-iT Picogreen kit (P7589, ThermoFisher) was used to quantify DNA content following the instructions of the manufacturer.

Statistical analyses

GraphPad Prism software (version 10.0.1) was used to carry out statistical analyses. Values presented in the graphs indicate the mean and standard deviation (SD) of at least three independent samples, unless stated otherwise. Data was compared using two-way ANOVA followed by Tukey's multiple comparisons test. To indicate statistically significant difference using *p* values, the following convention was used: * for $p < 0.05$, ** for $p < 0.01$, and *** for $p < 0.001$.

Results

hBM-MSC aggregate formation

In order to generate human bone marrow-derived MSC aggregates inside the spinner flask, $1x10^6$ cells/mL were cultured at a reduced speed to favour the spontaneous formation of aggregates (s_1, Figure 2). After checking aggregate size on a daily basis, as soon as aggregates of approximately

200µm diameter were formed, the speed was increased to avoid the formation of agglomerates (s_2, Figure 2).

It was observed that high speeds (trial 3, Figure 2C) led to cell clustering without effective aggregation. On the contrary, at low speeds (trial 1, Figure 2A), hBM-MSCs formed irregular aggregates of varying sizes. In addition, compared to a slightly higher stirring rate (trial 2, Figure 2B), the aggregates seemed less compact. Hence, based on the shape and the degree of aggregate compaction observed visually in the second trial (Figure 2B), subsequent experiments were carried out using these specific stirring rates.

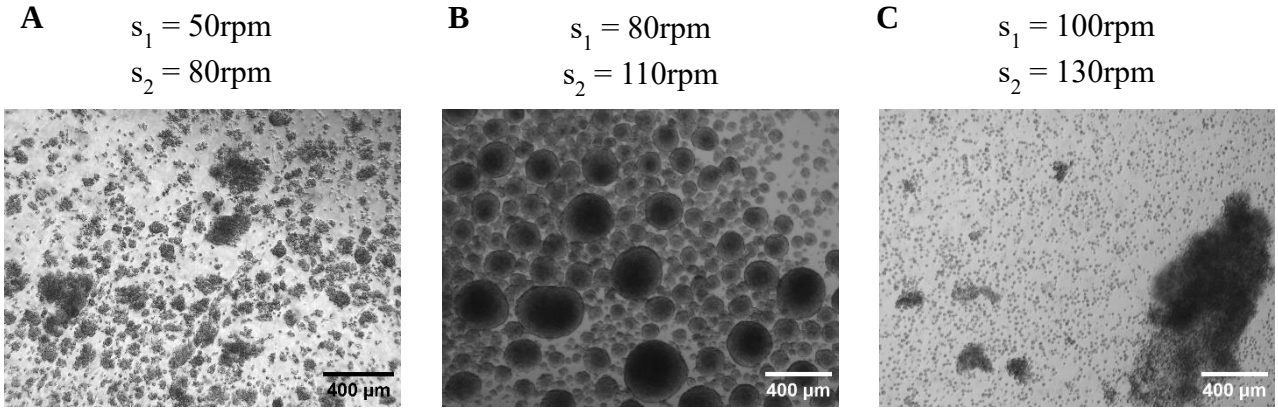

Figure 2. Assessment of the most favourable stirring rate for spontaneous hBM-MSC aggregate formation in dynamic culture. Brightfield pictures were taken at day 2 of culture. Speed 1 (s_1) was used during aggregate formation. Speed 2 (s_2) was used to avoid agglomeration once the hBM-MSC aggregates were formed. **(A)** Trial 1. **(B)** Trial 2. **(C)** Trial 3.

Formation of hBM-MSC aggregates in static and dynamic culture

Following the selection of the optimal stirring rate for self-aggregation of hBM-MSCs, subsequent experiments were conducted over longer culture periods. For these trials, spinner flasks were seeded with a cell density of $1x10^6$ cells/mL, whereas 96 well-plates contained $1x10^5$ cells per well.

After 21 days of culture, hBM-MSCs from donor 55 and 53 successfully formed aggregates, both in dynamic and static cultures (Figure 3A, Figure 4A). For both donors, the mean of the projected areas of aggregates obtained dynamically tended to increase during the first two weeks of culture (Figure 3B, Figure 4B). In the case of statically cultured aggregates, only a significant increase in size was observed for donor 53 during the first 4 days of culture ($p < 0.001$)(Appendix, Figure S1). It should be noted that, although there was a tendency for aggregate size to increase during the following days in the static culture, these changes were not statistically significant. Moreover, static culture with 50% medium changes presented similar results as the static culture with full medium changes (Figure 4B).

But what is of real importance is the notable contrast in variability between the dynamic and static cultures. The coefficient of variation (CV) within the static culture remained below 5% at most timepoints for both donors. Only on day 4 for donor 55 and on day 21 for both donors the CV surpassed 5% but remained below 10% (Figure 3D, Figure 4D). This low deviation of the results from the mean underscored the consistency of this culture system. As a matter of fact, 50% medium changes in the static culture showed the same outcome than full medium changes for donor 53 (Figure 4D), demonstrating that variations in this regard may not be influenced by the concentration

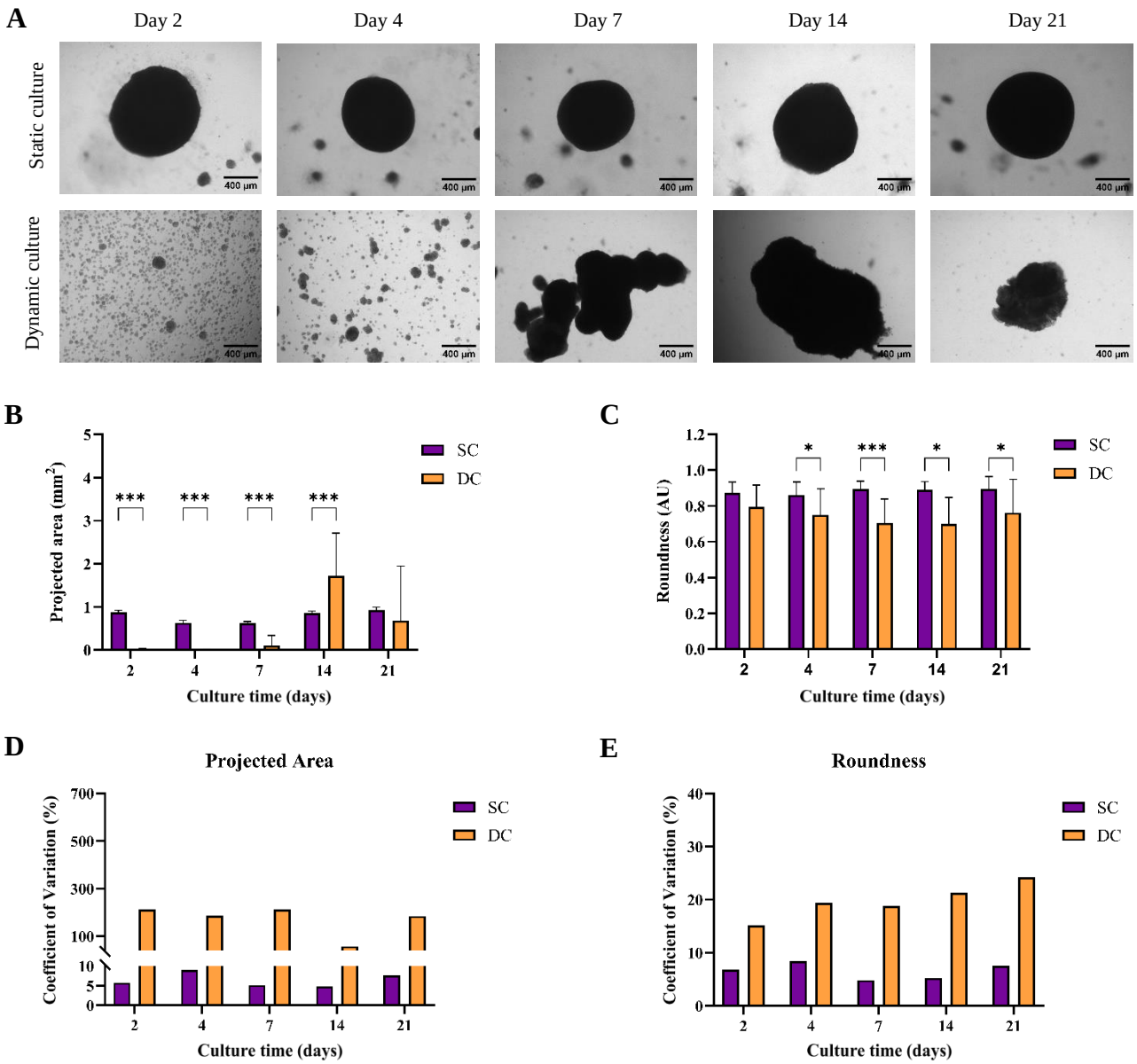

Figure 3. Culture of hBM-MSC aggregates from donor 55 in dynamic and static conditions. **(A)** Brightfield images of hBM-MSC aggregates from day 2 to day 21 of culture. **(B)** Averaged projected area of hBM-MSC aggregates at different timepoints. Comparison between culture systems. **(C)** Averaged roundness values of hBM-MSC aggregates. Comparison between culture systems. A perfect circle is indicated by 1.0, whereas lower values represent more elongated or irregular shapes. **(D)** Coefficient of variation (%) of the projected area of hBM-MSC aggregates at different timepoints. **(E)** Coefficient of variation of the roundness values of hBM-MSC aggregates at different timepoints. SC: static culture, DC: dynamic culture. The height of a bar represents the mean. The vertical lines represent the standard deviation (SD). Asterisks are used to denote significance (*p < 0.05, **p < 0.01, ***p < 0.001).

of the medium components. In contrast, aggregate size in dynamic culture of donor 55 exhibited a CV hovering around 200% at different timepoints (Figure 3D), with the exception of day 14 (CV = 57%). Similarly, for donor 53 the CV ranged from 138% (on day 21) to 669% (on day 14), remaining above 200% at the other timepoints (Figure 4D). These findings emphasised the high variation in size of the aggregates formed dynamically. As a result, a relevant comparison between the projected areas of the aggregates from both culture systems was not possible.

On the other hand, the microscopic images revealed that, for both donors, the aggregates resulting from the dynamic culture exhibited more irregular morphologies compared to the nearly circular shapes of the aggregates formed statically (Figure 3C, Figure 4C). Upon analysis of these microscopic images, our findings revealed variations in the roundness values of statically cultured

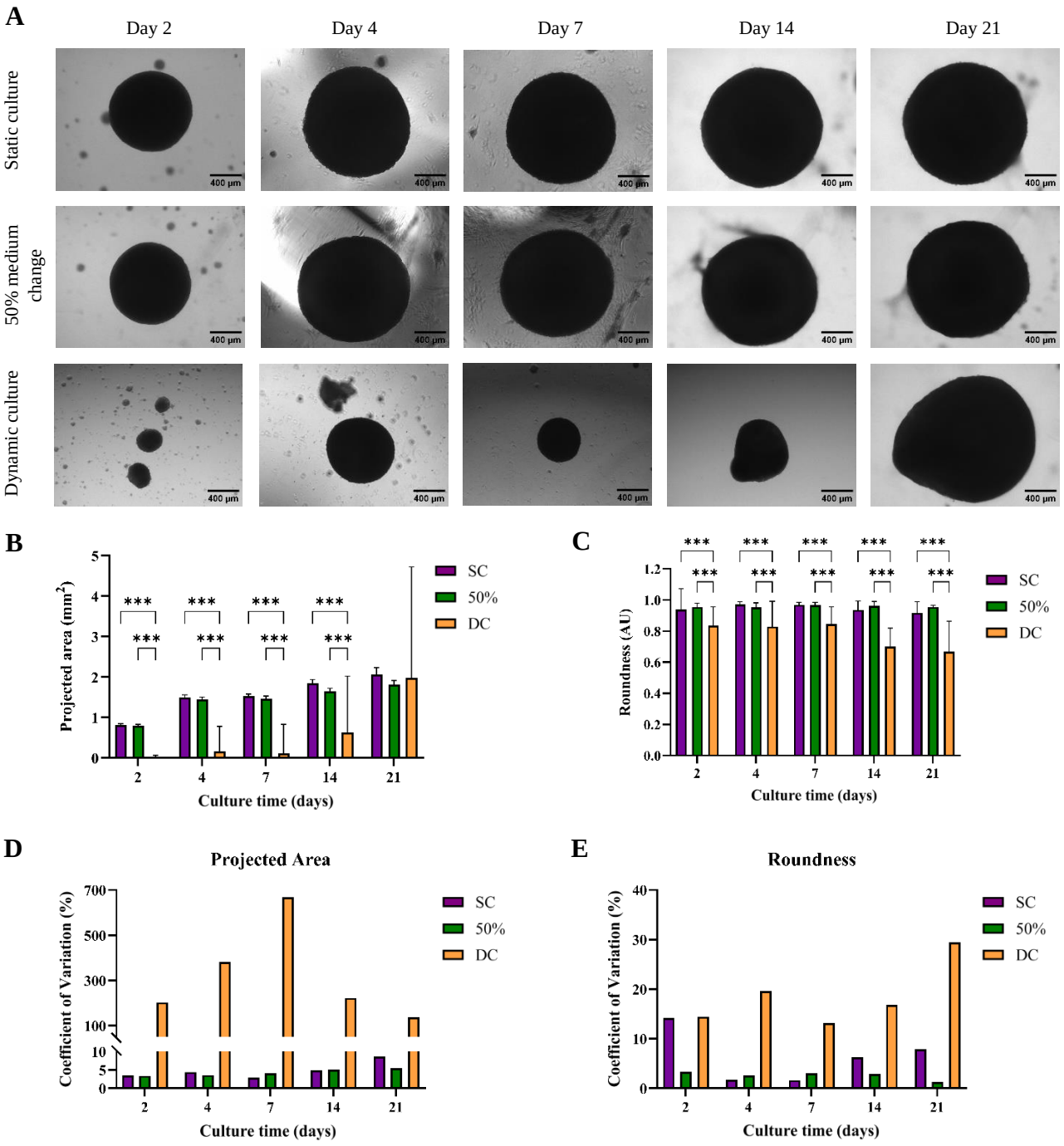

Figure 4. Culture of hBM-MSC aggregates from donor 53 in dynamic and static conditions. **(A)** Brightfield images of hBM-MSC aggregates from day 2 to day 21 of culture. **(B)** Averaged projected area of hBM-MSC aggregates at different timepoints. Comparison between culture systems. **(C)** Averaged roundness values of hBM-MSC aggregates. Comparison between culture systems. A perfect circle is indicated by 1.0, whereas lower values represent more elongated or irregular shapes. **(D)** Coefficient of variation (%) of the projected area of hBM-MSC aggregates at different timepoints. **(E)** Coefficient of variation of the roundness values of hBM-MSC aggregates at different timepoints. SC: static culture, DC: dynamic culture. 50%: static culture where half medium changes were performed. The height of a bar represents the mean. The vertical lines represent the standard deviation (SD). Asterisks are used to denote significance (*p < 0.05, **p < 0.01, ***p < 0.001).

aggregates, ranging from 0.861 ± 0.073 (mean ± standard deviation) to 0.896 ± 0.067 for donor 55 (Appendix, Table VII), and from 0.916 ± 0.072 to 0.971 ± 0.017 for donor 53 (Appendix, Table XI). Despite this range, the values from both donors approached the upper limit of 1.0, suggesting that these aggregates exhibited shapes that were relatively close to perfect circles. In addition, the shape of the statically cultured aggregates resulting from half medium changes resembled to those of the full medium changes, showing a roundness not lower than 0.953 ± 0.029 (Appendix, Table XI). This

suggested that 50% medium changes had no observable effects in the shape of the hBM-MSC aggregates formed statically.

In contrast, dynamically cultured aggregates displayed a wider range of roundness values. For donor 53, these values extended from 0.668 ± 0.197 to 0.844 ± 0.111 (Appendix, Table VII), while in the case of donor 53 the range extended from 0.699 ± 0.149 to 0.795 ± 0.121 (Appendix, Table XI). These findings corroborated that in dynamic culture a broader spectrum of aggregate shapes was observed. These variations were not only perceived across different days within the same culture system, but also within the same day. For both donors, dynamic culture resulted in CV values ranging from 13% to 30% across different timepoints (Figure 3E, Figure 4E). On the contrary, CV values of statically cultured aggregates remained below 10%, with the exception of day 2 for donor 53 (CV = 14%). This demonstrated the challenge for the dynamic culture to achieve a level of consistency comparable to that observed in static culture.

Viability of hBM-MSC aggregates in static and dynamic culture

During culture, aggregate samples were collected from both dynamic and static cultures aiming to assess the impact of the hydrodynamic conditions on the viability of the cells. The results from the viability assay revealed that, in the case of both donors, the amount of dead cells on the surface of the aggregates was relatively comparable to that of static culture (Figure 4A, B). This observation suggested that the shear stress generated by the hydrodynamic environment did not influence the viability of the cells present on the surface of the aggregates.

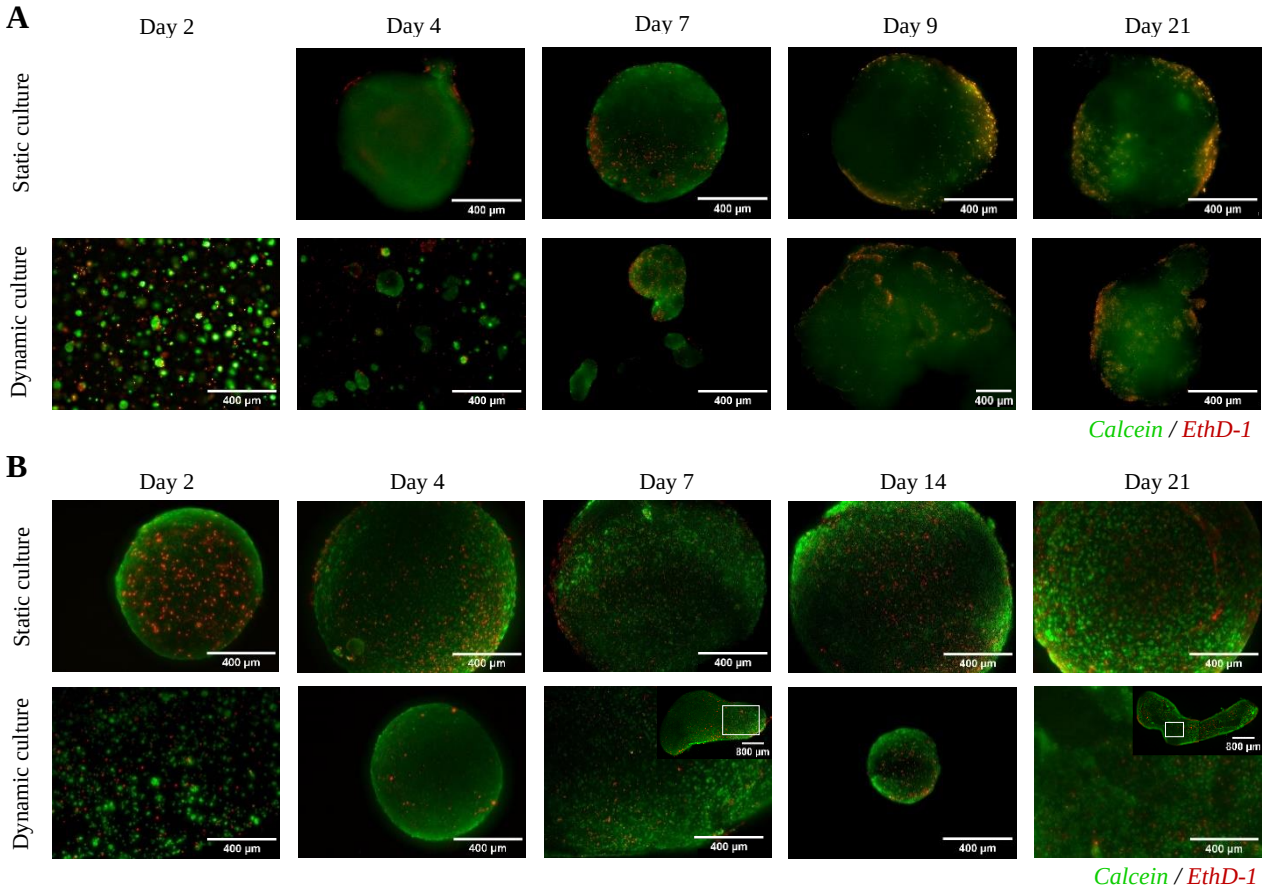

Figure 5. Cell viability assay of hBM-MSC aggregates. **(A)** Donor 55. The observed cell death on day 2 of dynamic culture is associated with diminished viability at the time of cell inoculation. Day 2 and Day 4 images from the dynamic culture flask represent cells and aggregates embedded in a collagen matrix. **(B)** Donor 53. Day 2 image from the dynamic culture represents cells and aggregates embedded in a collagen matrix. Calcein indicates viable cells. Ethidium homodimer (EthD-1) indicates dead cells.

In order to explore the possibility of necrotic core formation, aggregate sections were stained with DAPI to visualize the nuclei. Considering that aggregates in dynamic culture exhibited irregular morphologies, surface-to-centre distance was used to interpret the results by comparing them to the diffusion limit (150-200μm).

In relation to donor 55, both statically and dynamically cultured aggregates exhibited cell death when the distance from the aggregate surface to its centre exceeded 80μm, both on day 7 and day 21 of culture (Figure 6A). This distance was shorter than the diffusion limit, suggesting that the origination of necrotic cells may not be exclusively attributed to diffusion limitations. For donor 53, cell death was observable since day 7 in the aggregates from the two culture systems (Figure 6B). In both cases, dead cells were seen when the distance from the surface to the centre of the aggregates exceeded 300μm, thus surpassing the diffusion limit. Hence, despite the supposed advantages brought by the more efficient oxygen and nutrient delivery facilitated by the hydrodynamic environment of the spinner flask, cells still appeared to experience cell death.

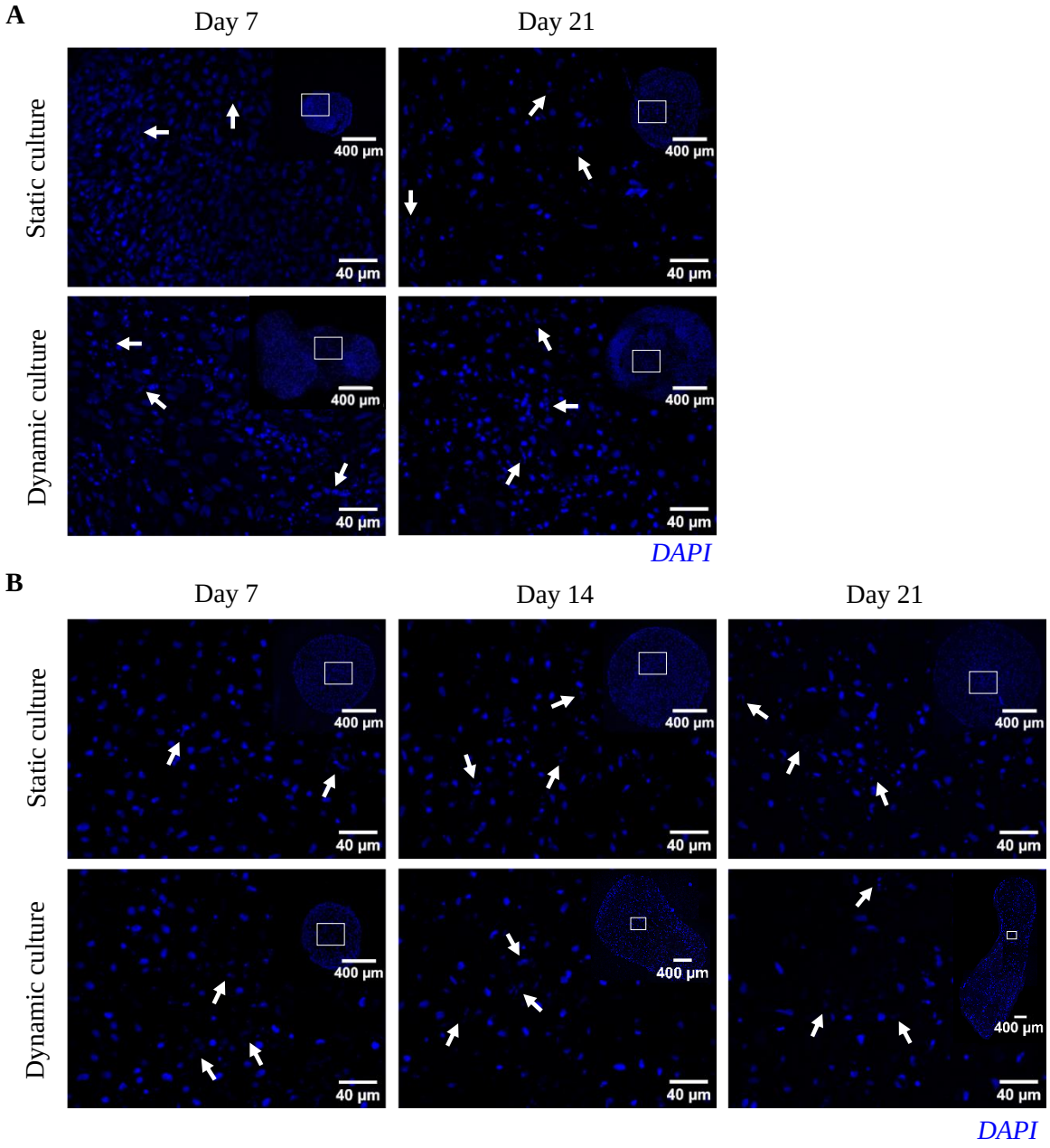

Figure 6. Cell viability assessment via nuclei visualization. **(A)** Donor 55. **(B)** Donor 53. DAPI stains cell nuclei, observed in blue. The arrows point to dead cells.

Chondrogenic differentiation of aggregates in static and dynamic culture

During the culture period, both donors underwent chondrogenic differentiation in static and dynamic culture. Positive Toluidine Blue and collagen II stainings indicated the presence of GAGs (Figure 7A, Figure 8A) and collagen type II (Figure 7D, Figure 8D), respectively. Moreover, cells apparently displayed chondrogenic morphology, where round chondrocytes which secreted these ECM components were inside the lacunae.

For donor 55, a faint purple staining could be observed on day 7 of both static and dynamic cultures (Figure 7A), indicating deposition of GAGs. However, collagen type II protein expression was only noticeable in static culture (Figure 7D). By day 21 of culture, differentiation became more apparent in both culture systems. In this case, GAG deposition, confirmed by the purple staining, and positive collagen II staining were visualized. In relation to this, quantitative assessment of GAGs over DNA revealed that GAG deposition in aggregates from dynamic culture was apparently reduced compared to static culture (Figure 7B), showing ratios of 1.328 ± 0.051 and 9.272 ± 0.755 respectively (Appendix, Table XIII).

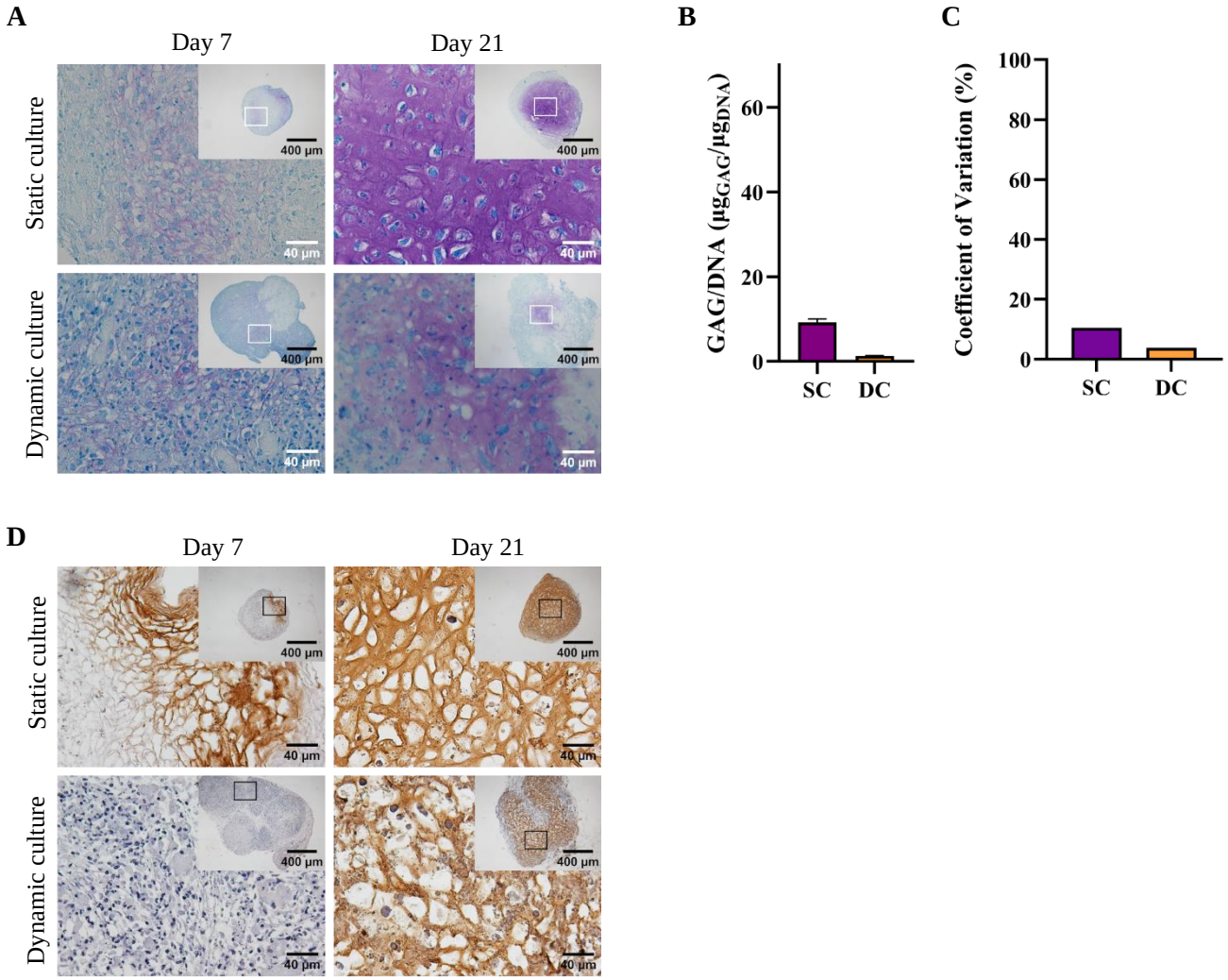

Figure 7. Characterization of chondrogenic differentiation of hBM-MSC aggregates from donor 55 over a period of 21 days. Sections of the aggregates were stained for different components of the extracellular matrix. **(A)** Toluidine Blue was used to stain glycosaminoglycans (GAGs), showed in purple, and Fast Green was used to stain collagenous fibres and cytoplasm, showed in blue. **(B)** Quantification of GAGs (µg/aggregate) normalized to DNA (µg/aggregate). The only timepoint available is day 21. **(C)** Coefficient of variation (%) of the GAG-to-DNA ratio on day 21 of culture. **(D)** Immunohistochemical staining used to visualize collagen type II, showed in brown. Cell nuclei were counterstained with Mayer's haematoxylin solution, showed in dark blue. SC: static culture, DC: dynamic culture. The height of a bar represents the mean. The vertical lines represent the standard deviation (SD).

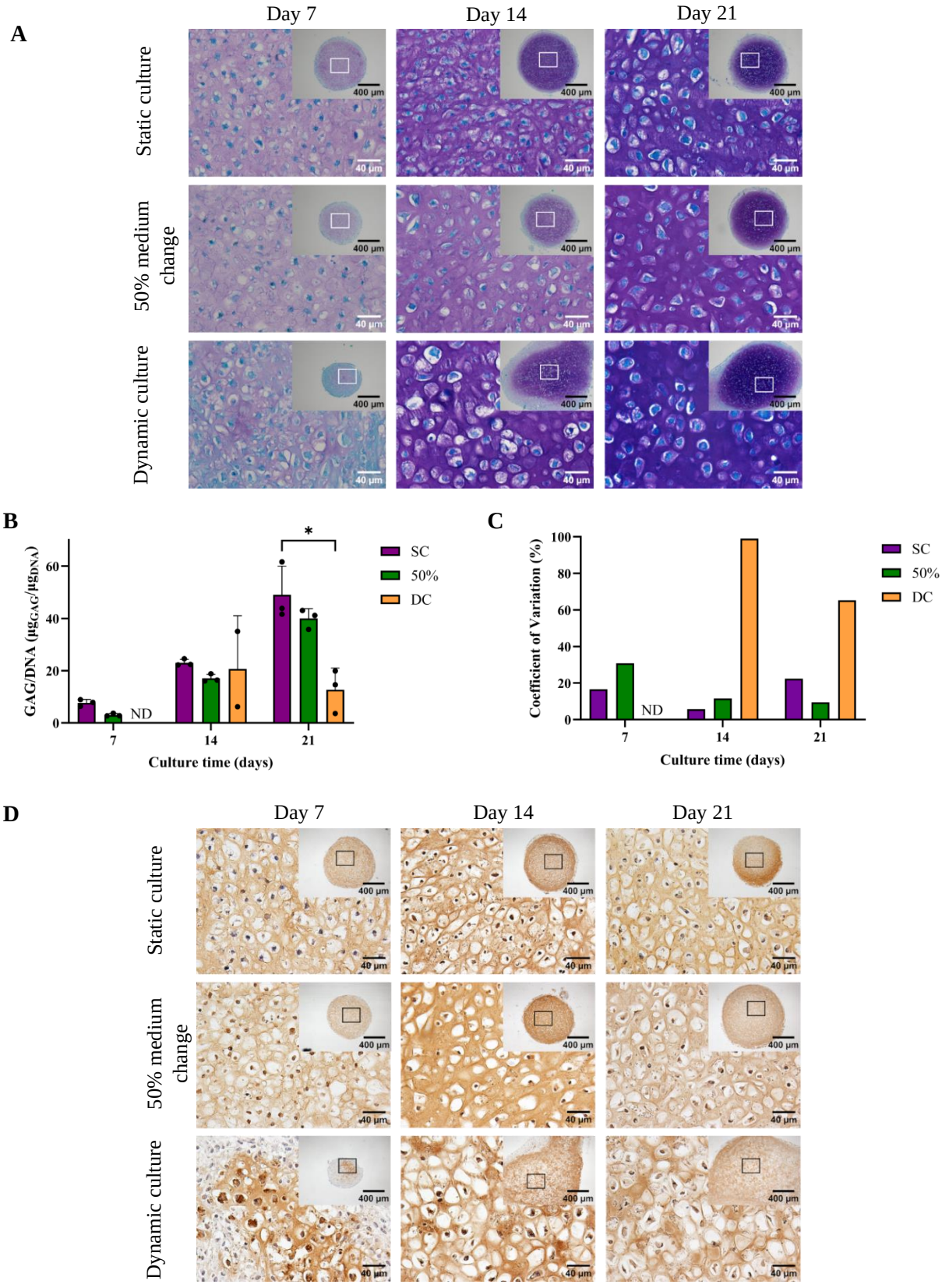

Figure 8. Characterization of chondrogenic differentiation of hBM-MSC aggregates from donor 53 over a period of 21 days. Sections of the aggregates were stained for different components of the extracellular matrix. **(A)** Toluidine Blue was used to stain glycosaminoglycans (GAGs), showed in purple, and Fast Green was used to stain collagenous fibres and cytoplasm, showed in blue. **(B)** Quantification of GAGs (µg/aggregate) normalized to DNA (µg/aggregate). Only two independent samples from the dynamic culture on day 14 were detectable. **(C)** Coefficient of variation (%) of the GAG-to-DNA ratio over the culture period. **(D)** Immunohistochemical staining used to visualize collagen type II, showed in brown. Cell nuclei were counterstained with Mayer's haematoxylin solution, showed in dark blue. SC: static culture, DC: dynamic culture, 50%: static culture where half medium changes were performed, ND: non detectable. The height of a bar represents the mean. The vertical lines represent the standard deviation (SD). Asterisks are used to denote significance (*p < 0.05, **p < 0.01, ***p < 0.001).

In contrast, donor 53 displayed signs of chondrogenic differentiation as early as day 7. In this case, Toluidine Blue and collagen II stainings were evenly distributed throughout the statically cultured aggregates (Figure 8A, D), where collagen II staining correlated with GAG deposition. Aggregates cultured dynamically exhibited purple staining in certain areas, correlating with collagen II staining and being more intense than those of donor 55. As the culture period progressed, GAG deposition seemed to intensify in both types of culture. These observations were corroborated by quantification data of GAGs over DNA, which showed a gradual increase in these values over time (Figure 8B). Interestingly, on day 21 of culture the aggregates obtained dynamically exhibited a significant lower GAG-to-DNA ratio in comparison to the ones obtained statically ($p < 0.035$), being 12.695 ± 8.285 and 49.017 ± 10.999, respectively (Appendix, Table XV). It is important to mention that 50% medium changes apparently showed reduced GAG-to-DNA ratios in comparison to full medium changes, being 39.977 ± 3.754 on day 21 (Appendix, Table XV). However, this decrease was not statistically significant, therefore indicating that this medium change regime may not induce significant alterations in chondrogenic differentiation in this culture system.

As in the case of aggregate size and shape, variability in chondrogenic differentiation was also observable. While the coefficient of variation (CV) for chondrogenesis in aggregates cultured statically stood at 6% on day 14 and 22% on day 21, aggregates cultured dynamically exhibited substantially higher CV values, being 99% on day 14 and 65% on day 21 (Figure 8C). This considerable variation in dynamic culture may be attributed to the uneven chondrogenesis among aggregates. Some aggregates demonstrated consistent differentiation throughout their structure, excluding the edges, whereas others displayed limited regions of GAG deposition and collagen II protein expression (Appendix, Figure S3). This event emphasised that, while static culture did exhibit some inconsistencies in chondrogenesis across aggregates, they were intensified in the dynamic culture. In conclusion, the hydrodynamic environment could be altering cell differentiation.

Adhesion molecule expression during 3D culture

To assess whether the hydrodynamic environment could affect the expression or distribution of adhesion molecules, thus influencing aggregate formation and compaction, an immunofluorescence analysis was performed. Specifically, the expression of neural cell adhesion molecule (NCAM) was examined.

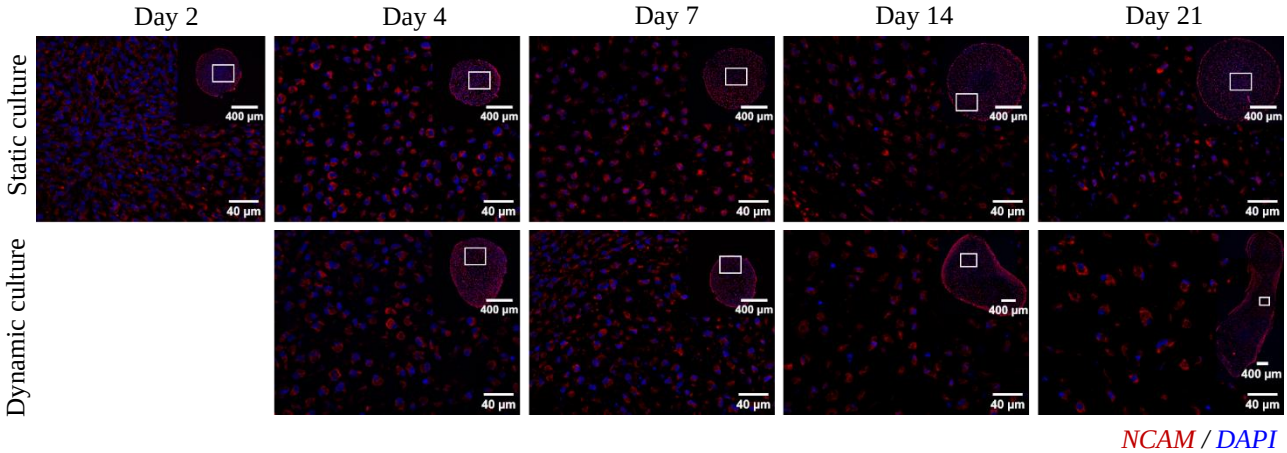

Figure 9. Evaluation of the protein expression of neural cell adhesion molecule (NCAM) via immunofluorescence. NCAM is observed in red. DAPI, which stains cell nuclei, is observed in blue.

The results of the immunofluorescence analysis revealed that NCAM was localised over the cell surface. However, no distinction was observed between static and dynamic conditions (Figure 9). As the aggregates began to undergo differentiation (evident from day 7 of culture, Figure 8A), the protein expression of NCAM appeared to decrease in both culture systems (Appendix, Figure S5), which may indicate a correlation between the process of cell differentiation and the expression of NCAM.

Discussion

The utilization of 3D static cultures has gained widespread recognition in the scientific community due to their ability to replicate the native tissue environment[9,11,12]. Likewise, there has been a growing interest in employing multipotent mesenchymal stromal cell (MSC) aggregates as a strategy for endochondral bone regeneration. The reason behind this occurrence is that MSCs have demonstrated spontaneous aggregation capacity and have been shown to undergo chondrogenic differentiation *in vitro*, ultimately leading to *in vivo* bone formation[6–8]. Nevertheless, several challenges accompany the static culture system, such as automation and scalability, among others[15]. In the pursuit of overcoming these challenges, dynamic culture has been suggested as a potential alternative to static culture. Previous reports have shown that the collision-based self-assembly of MSC aggregates is possible in dynamic cultures such as spinner flasks[11,13,21,30–32]. However, discrepancies in culture parameters prevail. Moreover, recent research has proven the potential of achieving chondrogenic differentiation of pre-assembled periosteum derived cell aggregates within a bioreactor setup. Yet, information regarding the possibility of collision-based formation and differentiation of human bone marrow-derived MSC (hBM-MSC) aggregates within the same bioreactor system using chondrogenic differentiation medium remains unknown. Hence, the aim of this report is to establish the feasibility of this concept.

Given that the stirring rate affects cell aggregation kinetics by influencing cell collisions[13,18], in this study different velocities were examined to determine the most favourable one for spontaneous hBM-MSC aggregate formation. It is essential to consider that collisions between aggregates might trigger agglomeration in the presence of low stirring rates[18]. Additionally, when the surface-to-centre distance of the aggregates exceeds the diffusion limit (150-200μm), there is a risk of necrotic core development[9,16,23,25]. This presents a challenge when aiming to culture viable cell aggregates without excessive agglomeration. To overcome these challenges, our strategy was based on setting a higher stirring speed (i.e., 80rpm, 110rpm, and 130rpm, depending on the trial) once the hBM-MSC aggregates were formed in the spinner flask.

Results indicated that for a cell density of $1x10^6$ cells/mL, high stirring rates (i.e., 110rpm) did not promote aggregate formation (Figure 2C). This could be due to shear stress generated by the hydrodynamic environment surpassing the adhesive strength between cell adhesion molecules, which as a result led to cell detachment from the aggregates[18]. Conversely, low stirring rates (i.e., 50rpm) resulted in random clustering of cells but no aggregate formation *per se* (Figure 2A), often generating a mass of cells accumulating at the bottom of the spinner flask. This observation, also reported in previous studies[13], suggested that the stirring rate was not enough to maintain cells in suspension and promote the necessary cell collisions for aggregate formation[15,18]. Interestingly, a stirring rate of 80 rpm supported aggregate formation (Figure 2B). This observation is in line with earlier studies that used a high initial cell density (i.e. $1x10^6$ cells/mL), which reported successful aggregation in spinner flasks at stirring rates of 70 and 80 rpm[11,21,31]. It is important to mention,

however, that these previous studies used expansion medium throughout the culture, namely αMEM supplemented with FBS. Hence, our study suggests that hBM-MSC aggregates can also form spontaneously when using chondrogenic differentiation medium.

After confirming the spontaneous formation of hBM-MSC aggregates in the spinner flask, a 21-day culture period was used to characterise changes in their features and to evaluate the chondrogenic differentiation of these aggregates in comparison to static culture. Results exhibited similarities between the aggregates from the two different donors. Notably, dynamic culture conditions significantly influenced aggregate size and morphology in comparison to static culture (Figure 3, Figure 4). On the contrary, 50% medium changes did not appear to affect these two variables (Figure 4), suggesting that the concentration of the medium components may not play an important role in aggregate shape and size. In addition, evident heterogeneity regarding these two variables was observed among aggregates within the spinner flask. In this context, literature showed disparity in results. For instance, Frith *et al*. and He *et al*. observed aggregates with regular spheroidal shapes[12,13], while Loverdou *et al*. and Miranda *et al*. reported variations in aggregate circularity[4,11]. However, a common thread across previous studies was that the projected area of the aggregates remained below 0.100mm^2. To be more precise, the projected areas previously documented ranged from 0.005mm^2, reported by He *et al*., to 0.096mm^2, reported by Bhang *et al*.[4,11–13,21,30,32], whereas the projected area of the aggregates in our study ranged from 0.002mm^2 to 4.756mm^2 (donor 55) and 8.124mm^2 (donor 53)(Appendix, Table V and Table IX, respectively). These different findings could be attributed to variations in experimental parameters, such as cell source, bioreactor setup, culture medium composition, initial cell density, and stirring rate. Interestingly, shear stress was reported to modulate the shape of chondrocytes cultured in a dish[36]. Considering that the shear stress within the spinner flask is heterogeneous[33,34], we could hypothesize that this non-uniform mechanical stimulus could result in differential compaction and deformation of the aggregates[18]. Thus, explaining the deviations from the expected spheroidal shape found in our study. On the other hand, the large projected area of our aggregates could be attributed to shear stress failing to surpass the adhesive strength of molecules involved in both ECM-cell and cell-cell interactions[18]. To confirm this, computational models focused on the self-assembly and culture of hBM-MSC aggregates would provide further insight into this matter. These findings highlight the influence of culture conditions on the characteristics of the aggregates. The challenges involved in obtaining consistent results using a dynamic culture system are demonstrated by the wider range of values of aggregate projected area and roundness displayed in comparison to static culture. In consequence, results underscore the need for optimising the dynamic culture setup in order to create a more consistent and reliable protocol.

In terms of viability, despite presumed more efficient diffusion of oxygen and nutrients due to the hydrodynamic environment, aggregates from donors 55 and 53 cultivated under dynamic conditions displayed signs of cell death when the distance from the surface to the centre exceeded 80μm and 300μm, respectively (Figure 6). These observations correlate with results from the static culture configuration and is evident across the different timepoints for both culture systems and donors. The cell death observed in donor 53 could be explained by the surface-to-centre distance exceeding the diffusion limit (150-200μm). This finding is further supported with prior research that indicated the absence of necrotic cores within dynamically cultured aggregates with surface-to-centre distances smaller than 150μm[4,12,21]. This suggests that the large size of our aggregates could indeed be a challenge to the viability of the cells. Regarding donor 55, the presence of dead cells could be related to the reduced cell viability observed during cell expansion phase. Nonetheless, it is essential to further analyse this specific donor to gain a more comprehensive understanding of the underlying factors contributing to the observed cell death. On the other hand, cells located on the surface of the

aggregate exhibited comparable viability in both culture systems for both donors (Figure 5). This observation may confirm that shear stress resulting from the hydrodynamic environment at stirring rates of 80 and 110rpm may not be the primary contributor to cell death.

In our study, chondrogenic differentiation of hBM-MSC aggregates within dynamic culture configuration was also assessed. Toluidine Blue and collagen type II staining results seemed to confirm chondrogenesis in hBM-MSC aggregates from donor 55 and 53 (Figure 7A, D, Figure 8A, D). This outcome was further reinforced by quantitative assessments (Figure 7B, Figure 8B). Notably, even with 50% medium changes, GAG over DNA levels remained comparable to full medium changes, suggesting that the process of chondrogenic differentiation is relatively robust to changes in this particular experimental setup (Figure 8B). Nevertheless, dynamically cultured aggregates appeared to exhibit reduced GAG deposition compared to static culture at day 21 for both donors. What is more important, heterogeneity was observed both between and within aggregates cultured dynamically, but not in the aggregates cultured statically. This heterogeneity found within hBM-MSC aggregates, regardless the size (Appendix, Figure S3), differs from prior reports which suggested that smaller aggregates maintain homogeneity in chondrogenesis[4,13]. A reasonable explanation for this heterogeneity is founded on the fact that, despite being designed to enhance oxygen and nutrient transfer, the spinner flask could introduce variations in the availability of these molecules across aggregates of different sizes[10], which may in turn lead to differences in chondrogenic differentiation. In addition, hBM-MSC aggregates in the dynamic culture displayed varying cellular densities and cell distribution. Consequently, this could impact nutrient diffusion, signalling molecule distribution, and cell-cell interactions[10], resulting in different responses across the aggregate and, as a result, in uneven differentiation. This heterogeneous chondrogenesis within the aggregates may explain the variation in the quantification of GAG over DNA in comparison to the static culture (Figure 7C, Figure 8C). All in all, dynamic culture complex microenvironment seemed to influence chondrogenic differentiation of aggregates in comparison to static conditions. Nonetheless, the foundations of the observed heterogeneity remain unclear.

To unravel the factors contributing to the observed heterogeneity both among and within aggregates, creating microenvironmental maps comes out as a promising solution. This approach could help in elucidating the spatial distribution of oxygen, nutrients, and signalling molecules that affect cellular behaviour[10], correlating the results with the differentiation outcomes. Complementary to this, computational analysis could also be conducted to understand *in silico* the distribution of molecules during the culture of hBM-MSC aggregates. Additionally, this computational analysis could include the quantification of mechanical forces experienced by cells in different regions of the aggregates, potentially providing insights into their correlation with differentiation patterns. On top of that, single cell analysis via RNA-sequencing can provide information of the gene expression profiles of individual cells within an aggregate, which can help identify gene expression variability contributing to differentiation heterogeneity.

In a similar vein, a potential solution for addressing challenges observed in the spinner flask culture could be the use of Rho kinase (ROCK) inhibitors (e.g., Y-27632). Research has shown that these inhibitors can enhance cell viability[37,38], alter aggregate morphology, and promote chondrogenesis[39]. In 2018, Wang *et al*. demonstrated that ROCK inhibition led to the formation of less compact aggregates without affecting cell-cell adhesions[39]. As a result, transport of different molecules and metabolites was enhanced, which led to an enhanced chondrogenesis in static culture[39]. This inhibitor's effectiveness is further supported by its proven ability to increase viability of bovine corneal endothelial cell aggregates and salivary gland stem cells[37,38]. Hence, although the adoption of Rho kinase inhibitors may introduce increased process costs, their use within hBM-MSC

aggregate dynamic cultures could yield valuable benefits. By potentially preventing or reducing necrotic core formation and improving chondrogenesis, these inhibitors could offer the prospect of improving aggregate quality in terms of homogeneous chondrogenic differentiation.

It is important to mention that existing literature has postulated that dynamic culture, due to shear stress, may promote differentiation toward pre-hypertrophic phenotypes[4]. Although the morphology of the cells within the aggregates obtained dynamically in our study may align with this, since they appeared to be round in shape and located inside a large lacuna surrounded by the extracellular matrix, similar morphology was observed in static culture (Figure 7A, Figure 8A). Therefore, morphological inspection alone does not definitively establish whether dynamically cultured aggregates exhibited a more hypertrophic phenotype compared to those in static culture. Genetic analyses involving hypertrophy markers (e.g., collagen X, Indian hedgehog signalling molecule (IHH)), should be used for further confirmation.

There are several studies underlying the importance of adhesion molecules in aggregate formation and compaction[10,16,23,27,40]. Since cell-cell adhesion complexes are mechanosensitive[41], the hydrodynamic environment of the dynamic culture could affect the expression or distribution of adhesion molecules. NCAM is a transmembrane glycoprotein known for its role in promoting cell-cell adhesion and interactions[40,42]. In the context of hBM-MSCs aggregation, the adhesive properties of this molecule may contribute to the compaction and organization of hBM-MSCs within multicellular aggregates[27,40], facilitating cellular communication. Thus, our study aimed to assess whether any variabilities existed in the expression of the neural cell adhesion molecule (NCAM) which could contribute to the disparity observed in size, shape, and differentiation potential between dynamically cultured and statically cultured aggregates.

It is worth noting that, since neural cadherin (N-cadherin) is one of the most expressed cadherins in BM-MSCs[10], and it is involved in cell aggregation and compaction of aggregates[10,16,17,23], studying its protein expression during aggregation and differentiation in the spinner flask in comparison to static culture could be of interest. In our study, although N-cadherin was stained (Appendix, Figure S4), the information obtained was not useful due to bad resolution and background. Therefore, only NCAM protein expression was assessed.

Returning to NCAM protein expression, our findings indicate that it did not seem to be affected by the mechanical stimuli apported by the spinner flaks in comparison to static culture conditions in donor 53 (Figure 9). Nonetheless, to definitively confirm potential differences in the expression of this molecule and its cellular location, further gene expression analysis could be performed in addition to the immunofluorescence studies. Notably, our results appear to reveal a diminishing expression of NCAM as cells started their differentiation into chondrocytes. This is in line with existing literature, which noted a reduction in NCAM expression when differentiation into chondrocytes started[27]. Interestingly, previous reports have also demonstrated that this reduction in the expression of NCAM is related to hypertrophic differentiation[40,42], which is the next step in endochondral bone regeneration. Adding to this and as previously mentioned, preceding research has highlighted the upregulation of genes related to hypertrophy in dynamic culture[4].

Taken together, exploring the gene expression profiles of different adhesion molecules, chondrogenic markers, and hypertrophic markers provides the opportunity to study the impact of dynamic culture on aggregation and differentiation of hBM-MSC aggregates in contrast to static culture.

Conclusions

In this work, we investigated the feasibility of collision-based self-assembly of human bone marrow-derived mesenchymal stromal cell (hBM-MSC) aggregates and their subsequent chondrogenic differentiation within the same bioreactor setup using chondrogenic differentiation medium. Our study demonstrated that a stirring rate of 80 rpm could lead to spontaneous hBM-MSC aggregate formation and confirmed chondrogenesis through a 21-day culture at 110rpm. The non-uniform mechanical stimuli provided by the hydrodynamic environment could be responsible for the differences in aggregate size, shape, and chondrogenic differentiation in comparison to static culture. Remarkably, our results highlighted challenges in maintaining the viability of large aggregates and revealed heterogeneity in chondrogenesis among and within dynamically cultured aggregates. To achieve the level of consistency and reliability demonstrated by static culture, future optimization of the dynamic culture setup is needed. However, prior to this optimization a comprehensive understanding of the underlying causes of the variability is required. Techniques such as microenvironmental mapping, computational analyses, or gene/protein expression profiling offer a promising approach for overcoming these challenges and advancing the efficacy of the dynamic culture system. Furthermore, we studied the role of adhesion molecules, particularly neural cell adhesion molecule (NCAM), in aggregate formation. While the mechanical stimuli of dynamic culture did not significantly affect NCAM expression, its reduction during chondrogenic differentiation aligns with existing literature and points at hypertrophic differentiation. Therefore, investigating the expression profiles of various molecules would offer valuable insights into the effects of dynamic culture on the aggregation and differentiation of hBM-MSC aggregates when compared to static culture.

In conclusion, this proof of concept demonstrates the feasibility of achieving spontaneous aggregate formation and its subsequent chondrogenic differentiation within the spinner flask system. Elucidating the molecular basis for the heterogeneity encountered in dynamically cultured aggregates could provide insights into enhancing the system for better outcomes concerning viability and differentiation capacity of hBM-MSC aggregates. Besides, working on the optimization of this culture system could offer valuable benefits for automation and upscaling, as it decreases manual intervention and workload associated with medium changes. This reduction in handling not only would minimize contamination risks, but also would align with good manufacturing practice (GMP) standards, ultimately facilitating clinical translation.

Bibliography

1. Gawlitta, D. *et al.* Modulating Endochondral Ossification of Multipotent Stromal Cells for Bone Regeneration. *Tissue Eng. Part B Rev.* **16**, 385–395 (2010).
2. Mescher, A. L. *Junqueira's Basic Histology Text & Atlas*. (McGraw-Hill Education, 2018).
3. Tam, W. L. *et al.* Human pluripotent stem cell-derived cartilaginous organoids promote scaffold-free healing of critical size long bone defects. *Stem Cell Res. Ther.* **12**, 513 (2021).
4. Loverdou, N. *et al.* Stirred culture of cartilaginous microtissues promotes chondrogenic hypertrophy through exposure to intermittent shear stress. *Bioeng. Transl. Med.* **8**, e10468 (2023).
5. Viswanathan, S. *et al.* Mesenchymal stem versus stromal cells: International Society for Cell & Gene Therapy (ISCT®) Mesenchymal Stromal Cell committee position statement on nomenclature. *Cytotherapy* **21**, 1019–1024 (2019).
6. Longoni, A. *et al.* Endochondral Bone Regeneration by Non-autologous Mesenchymal Stem Cells. *Front. Bioeng. Biotechnol.* **8**, (2020).
7. van der Stok, J. *et al.* Chondrogenically differentiated mesenchymal stromal cell pellets stimulate endochondral bone regeneration in critical-sized bone defects. *Eur. Cell. Mater.* **27**, 137–148; discussion 148 (2014).
8. Farrell, E. *et al.* In-vivo generation of bone via endochondral ossification by in-vitro chondrogenic priming of adult human and rat mesenchymal stem cells. *BMC Musculoskelet. Disord.* **12**, 31 (2011).
9. Kinney, M. A., Sargent, C. Y. & McDevitt, T. C. The Multiparametric Effects of Hydrodynamic Environments on Stem Cell Culture. *Tissue Eng. Part B Rev.* **17**, 249–262 (2011).
10. Sart, S., Tsai, A.-C., Li, Y. & Ma, T. Three-Dimensional Aggregates of Mesenchymal Stem Cells: Cellular Mechanisms, Biological Properties, and Applications. *Tissue Eng. Part B Rev.* **20**, 365–380 (2014).
11. Miranda, J. P. *et al.* The Secretome Derived From 3D-Cultured Umbilical Cord Tissue MSCs Counteracts Manifestations Typifying Rheumatoid Arthritis. *Front. Immunol.* **10**, (2019).
12. Frith, J. E., Thomson, B. & Genever, P. G. Dynamic Three-Dimensional Culture Methods Enhance Mesenchymal Stem Cell Properties and Increase Therapeutic Potential. *Tissue Eng. Part C Methods* **16**, 735–749 (2010).
13. He, H. *et al.* Dynamic formation of cellular aggregates of chondrocytes and mesenchymal stem cells in spinner flask. *Cell Prolif.* **52**, e12587 (2019).
14. Egger, D., Schwedhelm, I., Hansmann, J. & Kasper, C. Hypoxic Three-Dimensional Scaffold-Free Aggregate Cultivation of Mesenchymal Stem Cells in a Stirred Tank Reactor. *Bioengineering* **4**, 47 (2017).
15. Fuentes, P. *et al.* Dynamic Culture of Mesenchymal Stromal/Stem Cell Spheroids and Secretion of Paracrine Factors. *Front. Bioeng. Biotechnol.* **10**, (2022).

16. Kouroupis, D. & Correa, D. Increased Mesenchymal Stem Cell Functionalization in Three-Dimensional Manufacturing Settings for Enhanced Therapeutic Applications. *Front. Bioeng. Biotechnol.* **9**, (2021).

17. Ryu, N.-E., Lee, S.-H. & Park, H. Spheroid Culture System Methods and Applications for Mesenchymal Stem Cells. *Cells* **8**, 1620 (2019).

18. Moreira, JoséL., Cruz, P. E., Santana, P. C., Aunins, J. G. & Carrondo, M. J. T. Formation and disruption of animal cell aggregates in stirred vessels: Mechanisms and kinetic studies. *Chem. Eng. Sci.* **50**, 2747–2764 (1995).

19. Fu, L. *et al.* The Application of Bioreactors for Cartilage Tissue Engineering: Advances, Limitations, and Future Perspectives. *Stem Cells Int.* **2021**, e6621806 (2021).

20. Schneeberger, K. *et al.* Large-Scale Production of LGR5-Positive Bipotential Human Liver Stem Cells. *Hepatology* **72**, 257–270 (2020).

21. Santos, J. M. *et al.* Three-dimensional spheroid cell culture of umbilical cord tissue-derived mesenchymal stromal cells leads to enhanced paracrine induction of wound healing. *Stem Cell Res. Ther.* **6**, 90 (2015).

22. dos Santos, F. F., Andrade, P. Z., da Silva, C. L. & Cabral, J. M. S. Bioreactor design for clinical-grade expansion of stem cells. *Biotechnol. J.* **8**, 644–654 (2013).

23. Cui, X., Hartanto, Y. & Zhang, H. Advances in multicellular spheroids formation. *J. R. Soc. Interface* **14**, 20160877 (2017).

24. Tsai, A.-C., Liu, Y., Yuan, X., Chella, R. & Ma, T. Aggregation kinetics of human mesenchymal stem cells under wave motion. *Biotechnol. J.* **12**, 1600448 (2017).

25. Lin, R.-Z. & Chang, H.-Y. Recent advances in three-dimensional multicellular spheroid culture for biomedical research. *Biotechnol. J.* **3**, 1172–1184 (2008).

26. Cesarz, Z. & Tamama, K. Spheroid Culture of Mesenchymal Stem Cells. *Stem Cells Int.* **2016**, 9176357 (2016).

27. Hall, B. K. & Miyake, T. All for one and one for all: condensations and the initiation of skeletal development. *BioEssays* **22**, 138–147 (2000).

28. Sladkova, M. & De Peppo, G. M. Bioreactor Systems for Human Bone Tissue Engineering. *Processes* **2**, 494–525 (2014).

29. Stephenson, M. & Grayson, W. L. Recent advances in bioreactors for cell-based therapies. *F1000 Research* **7**, (F1000 Faculty Rev): 517 (2018).

30. Bhang, S. H. *et al.* Angiogenesis in ischemic tissue produced by spheroid grafting of human adipose-derived stromal cells. *Biomaterials* **32**, 2734–2747 (2011).

31. Kwon, S. H., Bhang, S. H., Jang, H.-K., Rhim, T. & Kim, B.-S. Conditioned medium of adipose-derived stromal cell culture in three-dimensional bioreactors for enhanced wound healing. *J. Surg. Res.* **194**, 8–17 (2015).

32. Allen, L. M., Matyas, J., Ungrin, M., Hart, D. A. & Sen, A. Serum-Free Culture of Human Mesenchymal Stem Cell Aggregates in Suspension Bioreactors for Tissue Engineering Applications. *Stem Cells Int.* **2019**, e4607461 (2019).

33. Ismadi, M.-Z. *et al.* Flow Characterization of a Spinner Flask for Induced Pluripotent Stem Cell Culture Application. *PLOS ONE* **9**, e106493 (2014).

34. Ghasemian, M. *et al.* Hydrodynamic characterization within a spinner flask and a rotary wall vessel for stem cell culture. *Biochem. Eng. J.* **157**, 107533 (2020).

35. Longoni, A. *et al.* Acceleration of Bone Regeneration Induced by a Soft-Callus Mimetic Material. *Adv. Sci.* **9**, 2103284 (2022).

36. Smith, R. L. *et al.* Effects of fluid-induced shear on articular chondrocyte morphology and metabolism in vitro. *J. Orthop. Res.* **13**, 824–831 (1995).

37. Guo, Y. *et al.* The Effects of ROCK Inhibitor Y-27632 on Injectable Spheroids of Bovine Corneal Endothelial Cells. *Cell. Reprogramming* **17**, 77–87 (2015).

38. Kim, K., Min, S., Kim, D., Kim, H. & Roh, S. A Rho Kinase (ROCK) Inhibitor, Y-27632, Inhibits the Dissociation-Induced Cell Death of Salivary Gland Stem Cells. *Molecules* **26**, 2658 (2021).

39. Wang, K.-C., Egelhoff, T. T., Caplan, A. I., Welter, J. F. & Baskaran, H. ROCK Inhibition Promotes the Development of Chondrogenic Tissue by Improved Mass Transport. *Tissue Eng. Part A* **24**, 1218–1227 (2018).

40. Tavella, S., Raffo, P., Tacchetti, C., Cancedda, R. & Castagnola, P. N-CAM and N-Cadherin Expression during in Vitro Chondrogenesis. *Exp. Cell Res.* **215**, 354–362 (1994).

41. De Belly, H., Paluch, E. K. & Chalut, K. J. Interplay between mechanics and signalling in regulating cell fate. *Nat. Rev. Mol. Cell Biol.* **23**, 465–480 (2022).

42. Cheng, B. *et al.* Neural cell adhesion molecule regulates chondrocyte hypertrophy in chondrogenic differentiation and experimental osteoarthritis. *Stem Cells Transl. Med.* **9**, 273–283 (2019).

Abbreviations

3D	Three-dimensional
bFGF	Basic fibroblast growth factor
BSA	Bovine serum albumin
CV	Coefficient of variation
DMMB	Dimethyl-methylene blue
ECM	Extracellular matrix
FBS	Foetal bovine serum
GAG	Glycosaminoglycan
GMP	Good manufacturing practice
hADSCs	Human adipose-derived stromal cells
hBM-MSCs	Human bone marrow-derived mesenchymal stromal cells
hUC-MSCs	Human umbilical cord tissue-derived mesenchymal stromal cells
hPDCs	Human periosteum derived cells
hSyF-MSCs	Human synovial fluid-derived mesenchymal stromal cells
MSC	Mesenchymal stromal cells
NCAM	Neural cell adhesion molecule
rBM-MSCs	Rabbit bone marrow-derived mesenchymal stromal cells
TGFβ1	Transforming growth factor beta 1

Appendix

Additional Materials and Methods

Chondrogenic differentiation assessment of hBM-MSC aggregates

In order to assess chondrogenic differentiation of dynamically cultured aggregates, a static control was needed. hBM-MSC aggregates of $2.5x10^4$ cells/aggregate, $5x10^4$ cells/aggregate, $7.5x10^4$ cells/aggregate, and $1x10^5$ cells/aggregate were cultured statically in a 96 U well suspension culture plate (650185, Greiner) for 21 days. This static culture control was only performed during trial 4 (donor 55). Since larger aggregates were found in the dynamic culture, a density of $1x10^5$cells/aggregate was chosen to compare chondrogenesis between the two culture systems, in both trials 4 and 5. After the 21-day culture, aggregates were collected and prepared for histological analysis.

Embedding and processing small sized aggregates for histology is a hard process. In order to facilitate this, hBM-MSC aggregates were first stained with eosin/formalin (ratio 1:1) overnight at room temperature after fixation in 4% formaldehyde solution. Once stained, aggregates were transferred to alginate 3% and were subsequently incubated for 15 minutes at room temperature with 10^2mM $CaCl_2$ in 3.7% formalin in order to crosslink. Posteriorly, dehydration, paraffin-embedding, and staining were performed as previously mentioned.

Antibody titration

For immunofluorescence analysis, antibodies needed to be titrated. Immunofluorescence staining steps were performed as previously mentioned. CD56 (NCAM) eFluor® 660 antibody (50-0565-80, clone 5tukon56, Invitrogen) and N-cadherin Alexa Fluor® 488 antibody (sc-59987, clone 13A9, Santa Cruz Biotechnology) were used. Dilutions of 1:20, 1:25, and 1:30 in 5% BSA/PBS of each antibody were tested. Nuclei were counterstained and coverslips were mounted using VECTASHIELD® HardSet Antifade Mounting Medium with DAPI (H-1500, Vector Laboratories). The immunofluorescence signals were imaged using a fluorescence microscope (Leica DMi8 with THUNDER Imaging System, Leica Microsystems).

Additional Results

Formation of hBM-MSC aggregates in static and dynamic culture

Table V. Averaged projected area values (mm^2) of hBM-MSC aggregates from donor 55. Results show mean ± standard deviation.

	Day 2	Day 4	Day 7	Day 14	Day 21
Static culture	0.877 ± 0.051	0.630 ± 0.056	0.628 ± 0.032	0.860 ± 0.041	0.922 ± 0.070
Dynamic culture	0.010 ± 0.021	0.009 ± 0.016	0.109 ± 0.232	1.726 ± 0.986	0.684 ± 1.258

Table VI. Coefficient of variation (%) for projected area values of hBM-MSC aggregates from donor 55.

	Day 2	Day 4	Day 7	Day 14	Day 21
Static culture	5.77	8.97	5.13	4.78	7.62
Dynamic culture	211	185	212	57.1	184

Table VII. Averaged roundness values (arbitrary units) of hBM-MSC aggregates from donor 55. Results show mean ± standard deviation.

	Day 2	Day 4	Day 7	Day 14	Day 21
Static culture	0.874 ± 0.060	0.861 ± 0.073	0.894 ± 0.043	0.889 ± 0.047	0.896 ± 0.067
Dynamic culture	0.795 ± 0.121	0.750 ± 0.133	0.705 ± 0.133	0.699 ± 0.149	0.763 ± 0.185

Table VIII. Coefficient of variation (%) for roundness values of hBM-MSC aggregates from donor 55.

	Day 2	Day 4	Day 7	Day 14	Day 21
Static culture	6.82	8.43	4.82	5.26	7.51
Dynamic culture	15.2	19.4	18.8	21.3	24.3

Table IX. Averaged projected area (mm^2) values of hBM-MSC aggregates from donor 53. Results show mean ± standard deviation.

	Day 2	Day 4	Day 7	Day 14	Day 21
Static culture	0.815 ± 0.028	1.491 ± 0.066	1.535 ± 0.045	1.850 ± 0.092	2.055 ± 0.176
50% medium change	0.802 ± 0.027	1.454 ± 0.053	1.471 ± 0.061	1.641 ± 0.083	1.817 ± 0.100
Dynamic culture	0.023 ± 0.046	0.162 ± 0.620	0.108 ± 0.721	0.626 ± 1.391	1.985 ± 2.733

Table X. Coefficient of variation (%) for projected area values of hBM-MSC aggregates from donor 53.

	Day 2	Day 4	Day 7	Day 14	Day 21
Static culture	3.47	4.42	2.92	4.96	8.58
50% medium change	3.41	3.62	4.14	5.05	5.50
Dynamic culture	202	382	669	222	138

Table XI. Averaged roundness values (arbitrary units) of hBM-MSC aggregates from donor 53. Results show mean ± standard deviation.

	Day 2	Day 4	Day 7	Day 14	Day 21
Static culture	0.938 ± 0.133	0.971 ± 0.017	0.969 ± 0.016	0.936 ± 0.059	0.916 ± 0.072
50% medium change	0.954 ± 0.032	0.955 ± 0.025	0.953 ±0.029	0.962 ± 0.028	0.955 ± 0.012
Dynamic culture	0.834 ± 0.120	0.828 ± 0.163	0.844 ± 0.111	0.700 ± 0.118	0.668 ± 0.197

Table XII. Coefficient of variation (%) for roundness values of hBM-MSC aggregates from donor 53.

	Day 2	Day 4	Day 7	Day 14	Day 21
Static culture	14.2	1.75	1.64	6.28	7.90
50% medium change	3.33	2.59	3.02	2.89	1.23
Dynamic culture	14.4	19.6	13.2	16.8	29.4

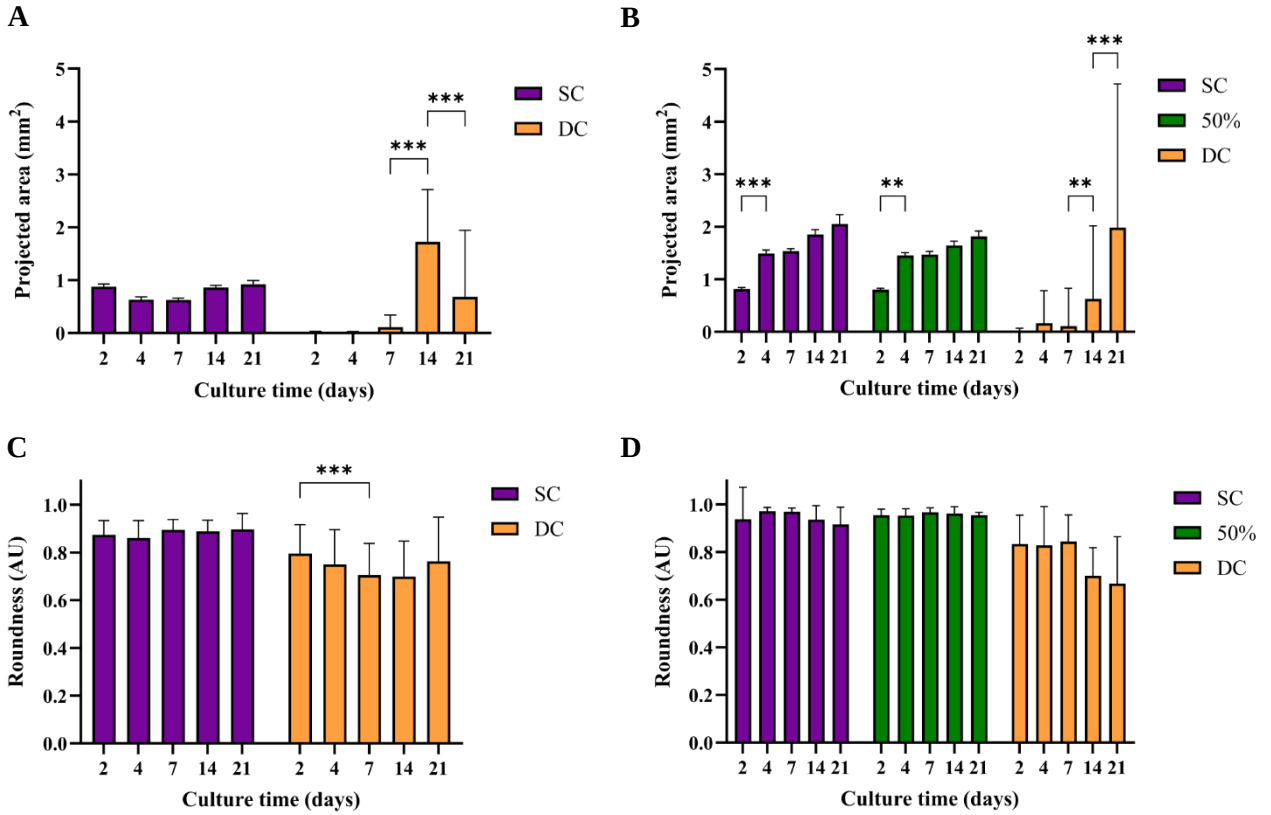

Figure S1. Culture of hBM-MSC aggregates from donor 55 and 53 in dynamic and static culture conditions. **(A)** and **(B)** Averaged projected area of hBM-MSC aggregates at different timepoints from donor 55 and 53, respectively. Comparison between days within the same culture system. **(C)** and **(D)** Averaged roundness values of hBM-MSC aggregates from donor 55 and 53, respectively. Comparison between days within the same culture system. A perfect circle is indicated by 1.0, whereas lower values represent more elongated or irregular shapes. SC: static culture, DC: dynamic culture, 50%: static culture where half medium changes were performed. The height of a bar represents the mean. The vertical lines represent the standard deviation (SD). Asterisks are used to denote significance (*p < 0.05, **p < 0.01, ***p < 0.001).

Chondrogenic differentiation of aggregates in static and dynamic culture

Table XIII. Averaged GAG/DNA values of hBM-MSC aggregates from donor 55. Results show mean ± standard deviation.

	Day 21
Static culture	9.776 ± 1.024
Dynamic culture	1.328 ± 0.051

Table XIV. Coefficient of variation (%) for GAG/DNA values of hBM-MSC aggregates from donor 55.

	Day 21
Static culture	10.5
Dynamic culture	3.86

Table XV. Averaged GAG/DNA values of hBM-MSC aggregates from donor 53. Results show mean ± standard deviation.

	Day 7	Day 14	Day 21
Static culture	7.712 ± 1.280	23.02 ± 1.316	49.02 ± 11.00
50% medium change	3.528 ± 1.086	17.70 ± 2.041	39.98 ± 3.754
Dynamic culture	Non detectable	20.61 ± 20.40	12.69 ± 8.285

Table XVI. Coefficient of variation (%) for GAG/DNA values of hBM-MSC aggregates from donor 55.

	Day 7	Day 14	Day 21
Static culture	16.6	5.72	22.4
50% medium change	30.8	11.5	9.39
Dynamic culture	Non detectable	99.0	65.3

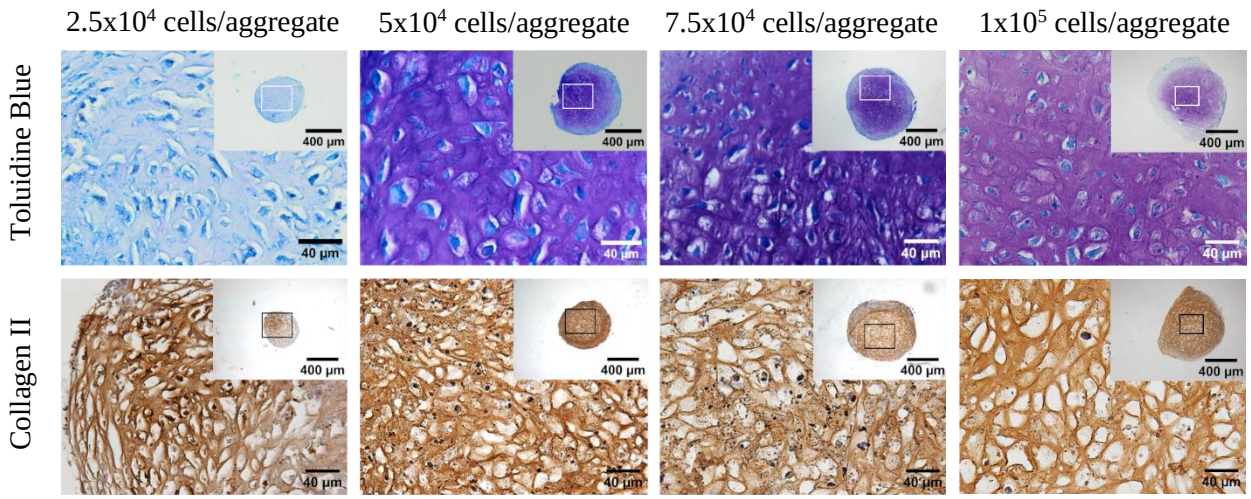

Figure S2. Chondrogenic differentiation assessment of statically cultured hBM-MSC aggregates from donor 55 (trial 4) on day 21 of culture. Toluidine Blue was used to stain glycosaminoglycans (GAGs), showed in purple, and Fast Green was used to stain collagenous fibres and cytoplasm, showed in blue. Immunohistochemical staining used to visualize collagen type II, showed in brown. Cell nuclei were counterstained with Mayer's haematoxylin solution, showed in dark blue.

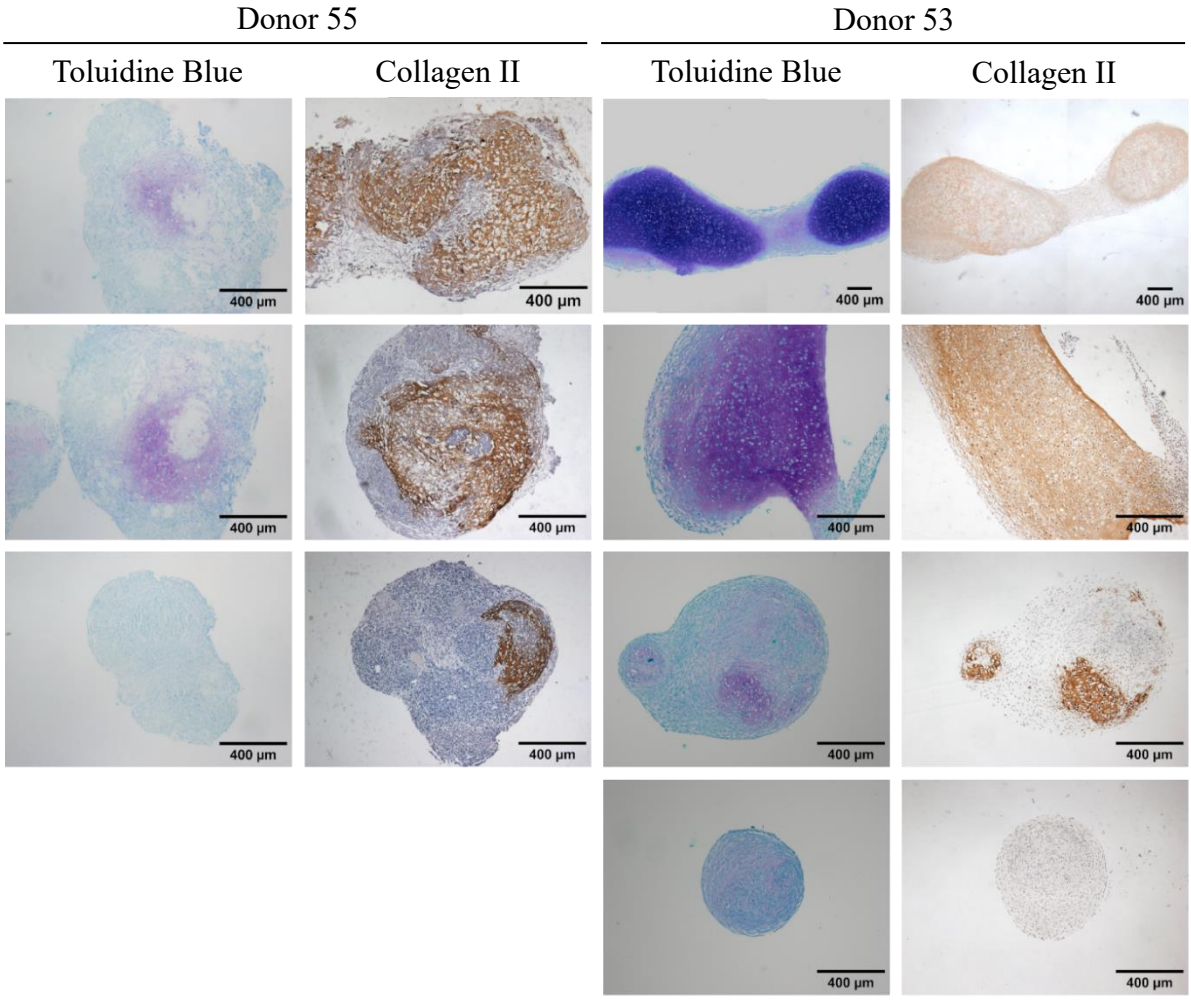

Figure S3. Chondrogenic differentiation of dynamically cultured hBM-MSC aggregates on day 21. Toluidine Blue was used to stain glycosaminoglycans (GAGs), showed in purple, and Fast Green was used to stain collagenous fibres and cytoplasm, showed in blue. Immunohistochemical staining used to visualize collagen type II, showed in brown. Cell nuclei were counterstained with Mayer's haematoxylin solution, showed in dark blue.

Adhesion molecule expression during 3D culture

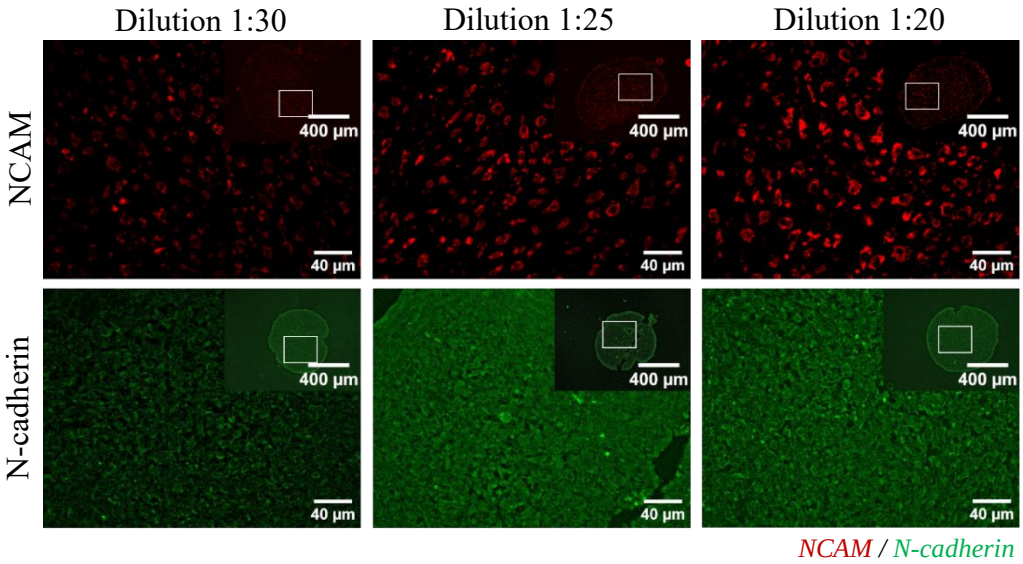

Figure S4. Titration of anti-NCAM and anti-N-cadherin antibodies. The 1:30, 1:25 and 1:20 dilutions are equivalent to antibody concentrations of 6µg/mL, 8µg/mL and 10µg/mL, respectively. NCAM is observed in red. N-cadherin is observed in green.

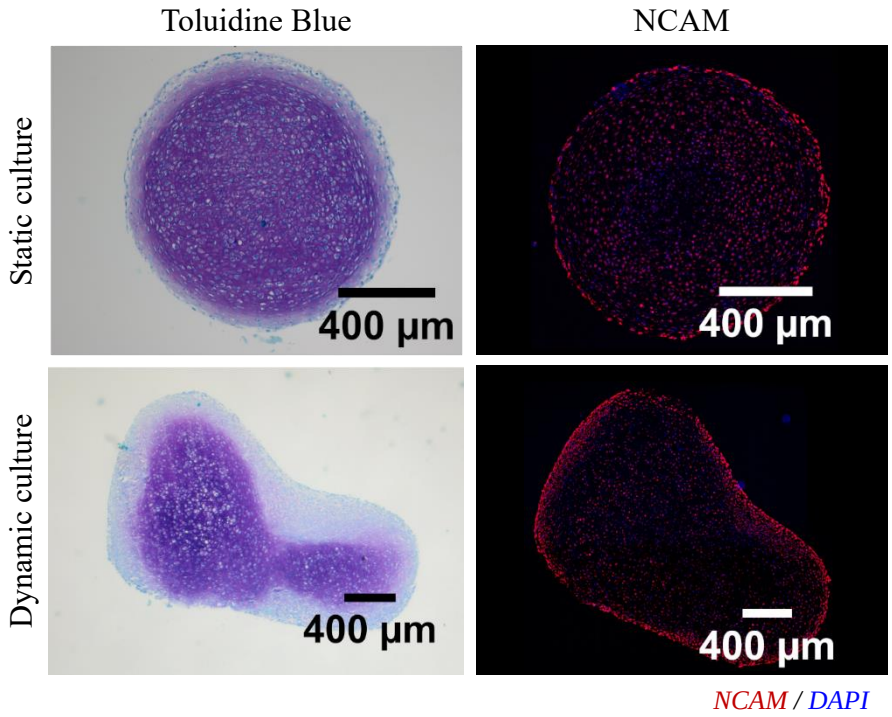

Figure S5. Visualization of the apparent reduction of NCAM protein expression after chondrogenic differentiation of the cells. Day 14 of culture. Toluidine Blue was used to stain glycosaminoglycans (GAGs), showed in purple, and Fast Green was used to stain collagenous fibres and cytoplasm, showed in blue. Immunohistochemical staining used to visualize collagen type II, showed in brown. Cell nuclei were counterstained with Mayer's haematoxylin solution, showed in dark blue. NCAM is observed in red. DAPI, which stains cell nuclei, is observed in blue.